
The Disparate Benefits of Deep Ensembles

Kajetan Schweighofer¹ Adrian Arnaiz-Rodriguez² Sepp Hochreiter^{1,3} Nuria Oliver²

¹ ELLIS Unit, LIT AI Lab, Institute for Machine Learning, JKU Linz, Austria

² ELLIS Alicante, Alicante, Spain

³ NXAI GmbH, Linz, Austria

{schweighofer, hochreit}@ml.jku.at, {adrian, nuria}@ellisalicante.org

Abstract

Ensembles of Deep Neural Networks, Deep Ensembles, are widely used as a simple way to boost predictive performance. However, their impact on algorithmic fairness is not well understood yet. Algorithmic fairness investigates how a model’s performance varies across different groups, typically defined by protected attributes such as age, gender, or race. In this work, we investigate the interplay between the performance gains from Deep Ensembles and fairness. Our analysis reveals that they unevenly favor different groups in what we refer to as a *disparate benefits* effect. We empirically investigate this effect with Deep Ensembles applied to popular facial analysis and medical imaging datasets, where protected group attributes are given and find that it occurs for multiple established group fairness metrics, including statistical parity and equal opportunity. Furthermore, we identify the per-group difference in predictive diversity of ensemble members as the potential cause of the disparate benefits effect. Finally, we evaluate different approaches to reduce unfairness due to the disparate benefits effect. Our findings show that post-processing is an effective method to mitigate this unfairness while preserving the improved performance of Deep Ensembles.

1 Introduction

Deep Ensembles (Lakshminarayanan et al., 2017) have demonstrated their efficacy as a simple and robust method to improve the performance of individual Deep Neural Networks (DNNs). Their superior performance has made them a popular choice for real-world applications (Bhusal et al., 2021; Dolezal et al., 2022), including high-stakes scenarios where the impact on people’s lives of machine learning supported decisions can be profound, such as in healthcare, education, finance or the law. In such applications, it is crucial to examine how these models perform across different groups that are defined by a protected attribute (e.g., gender, age, race, etc.) which is the focus of the field of Algorithmic Fairness (Barocas et al., 2023). Ensuring equitable operation of these models across protected groups is imperative, as they can significantly impact individuals and communities, potentially widening existing disparities if not adequately addressed. Although the differences in performance across protected groups (group fairness violations) of individual DNNs has been extensively studied (Zhang et al., 2018; Sagawa et al., 2020; Zhang et al., 2022; Arnaiz-Rodriguez & Oliver, 2024), the impact on fairness of ensembling these networks remains underexplored.

In this paper, our aim is to fill this gap by conducting an extensive empirical study of the fairness implications of Deep Ensembles, analyzing their underlying causes, and exploring mitigation strategies. Our empirical study is based on two popular facial analysis datasets and a widely used medical imaging dataset, each with multiple targets and protected group attributes. We evaluate a total of fifteen tasks across five different DNN model architectures and using three standard group fairness measures. Our analyses reveal that Deep Ensembles unevenly benefit different protected groups in what we refer to as the *disparate benefits* effect (c.f. Fig. 1). We further investigate the causes of this

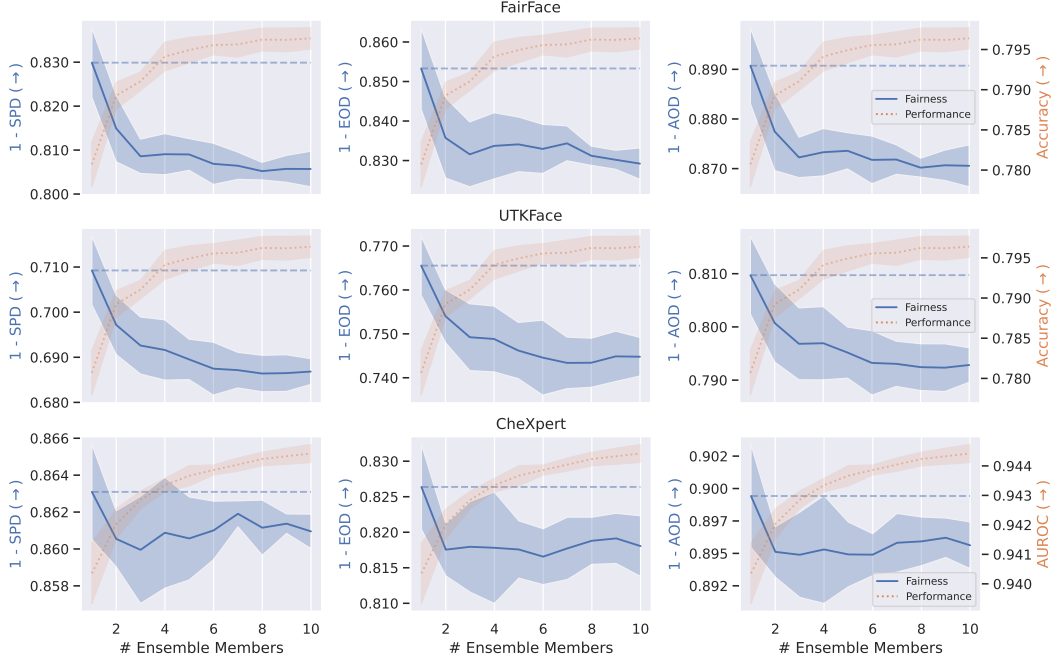


Figure 1: **Negative consequences of the disparate benefits effect of Deep Ensembles.** The performance increases, but the fairness decreases when more members are added to the ensemble. Performance is measured by accuracy (FairFace and UTKFace) and AUROC (CheXpert). Fairness is measured as 1-SPD, 1-EOD and 1-AOD, where SPD, EOD and AOD are common metrics capturing group fairness violations. The dashed blue line indicates the average fairness of individual ensemble members. Results for the FairFace and UTKFace datasets are obtained for target age and protected group attribute gender. Results for the CheXpert dataset are obtained for target no finding and protected group attribute age. Statistics are based on five independent runs (ResNet50).

disparate benefits effect, and find evidence that differences in the predictive diversity of ensemble members across groups are the reason why ensembling benefits groups differently. Finally, we explore potential approaches to mitigate the negative impact on fairness caused by the disparate benefits effect. We find that Deep Ensembles are more sensitive to the prediction threshold than individual models due to their improved calibration. This makes post-processing methods a suitable approach to mitigate the fairness violations. In fact, our results show that Hardt post-processing (Hardt et al., 2016) is very effective, yielding fairer predictions while preserving the improved performance of Deep Ensembles. In sum, the main contributions of this paper are three-fold:

1. We empirically analyze how the performance improvements of Deep Ensembles distribute across groups defined by protected attributes (Sec. 5). Our findings reveal that Deep Ensembles yield disparate benefits across groups, often benefiting the already advantaged group.
2. We investigate potential causes for the disparate benefits effect (Sec. 6). Our analysis suggests the per-group differences in the predictive diversity of ensemble members as an underlying factor.
3. We evaluate approaches to mitigate the negative impact of the disparate benefits effect (Sec. 7). We find that Deep Ensembles are more sensitive to the prediction threshold due to their improved calibration. Thus, Hardt post-processing (Hardt et al., 2016) is found to be very effective, ensuring more fair predictions while preserving the improved performance of Deep Ensembles.

2 Related Work

Algorithmic Fairness. Algorithmic fairness is defined using various ethical and legal concepts (Barocas & Selbst, 2016; Corbett-Davies et al., 2017; Binns, 2018), resulting in diverse statistical and causal notions of equality across tasks and contexts (Kusner et al., 2017; Mehrabi et al., 2021). We focus on group fairness metrics—statistical discrimination metrics for classification (Carey & Wu, 2023)—that measure error rate differences between groups defined by protected attributes (Hardt

et al., 2016; Zafar et al., 2017). Several metrics quantify group fairness by imposing independence conditions on the joint distribution of targets, predictions, and protected attributes (Barocas et al., 2023), capturing performance disparities due to varying input and target distributions among protected groups (Garg et al., 2020; Pombal et al., 2022). Consequently, a multitude of ML techniques have emerged over the past decade to promote group algorithmic fairness (Mehrabi et al., 2021) by modifying the data (pre-processing) (Kamiran & Calders, 2012; Arnaiz-Rodriguez & Oliver, 2024), the learning process (in-processing) (Agarwal et al., 2018; Jung et al., 2023); or the model’s decision rule (post-processing) (Hardt et al., 2016; Cruz & Hardt, 2024). In this paper, we focus on group algorithmic fairness and analyze the impact on group fairness of Deep Ensembles.

Deep Ensembles. Deep Ensembles (Lakshminarayanan et al., 2017) are known as a simple and effective method to boost the performance of DNNs and to estimate uncertainty (Ovadia et al., 2019; Ashukha et al., 2020; Schweighofer et al., 2023). They mostly rely on the stochasticity of the initialization and optimization procedure for diversity (Fort et al., 2019). However, obtaining more diverse Deep Ensembles is still an active area of research (Rame & Cord, 2021; Lee et al., 2023; Pagliardini et al., 2023). Furthermore, the exact mechanisms that yield the performance improvements observed in Deep Ensembles remain an open research question (Abe et al., 2022b; Jeffares et al., 2023; Abe et al., 2024). Prior work at the intersection of algorithmic fairness and ensembling has investigated the effect of model multiplicity (Marx et al., 2020; Coston et al., 2021; Black et al., 2022a,b; Long et al., 2023; Cooper et al., 2024), and has reported that ensembling decreases the multiplicity of predictions, thus being less arbitrary than individual models. Shallow model ensembles have been used to improve the fairness of outcomes (Kamiran & Calders, 2012), yet we are not aware of any work that has investigated the impact of Deep Ensembles on group fairness metrics.

The most closely related previous work to ours is Ko et al. (2023), which investigates the effect of Deep Ensembles on subgroup performance and served as an inspiration to our work. However, their focus and methodology are different from ours. For most of their experiments, the group variable of interest A is defined as a subset of the full target space \mathcal{Y} , *i.e.*, of the worst and best performing targets. In our experiments with real-world data, groups are defined by the values of a protected attribute, such as age, gender, or race. Furthermore, Ko et al. do not consider established group fairness measures as we do, focusing instead on per-group changes in accuracy. Finally, Ko et al. conclude that Deep Ensembles have exclusively positive impact, while we show that they can negatively affect group fairness. We investigate potential causes for this effect and analyze mitigation strategies that preserve fairness while maintaining the performance gains of the ensembles.

3 Background

We consider the canonical setting of binary classification with inputs $\mathbf{x} \in \mathbb{R}^D$, targets $y \in \{0, 1\}$, and group attributes $a \in \{0, 1\}$ defined according to protected or sensitive variables, such as gender, age, or race. Furthermore, we consider DNNs as the models to map an input \mathbf{x} to the 1-dimensional probability simplex $\Delta^1 = \{(s_0, s_1) \in \mathbb{R}^2 \mid s_0 \geq 0, s_1 \geq 0, s_0 + s_1 = 1\}$. We define this mapping as $f_{\mathbf{w}} : \mathbb{R}^D \rightarrow \Delta^1$ for a model with parameters \mathbf{w} . The output of this mapping defines the distribution parameters of the predictive distribution of the model, denoted by $p(y \mid \mathbf{x}, \mathbf{w})$. A training dataset $\mathcal{D} = \{(\mathbf{x}_j, y_j)\}_{j=1}^J$ is used to determine the model parameters by minimizing the cross-entropy loss. The final prediction \hat{y} is given by the argmax over the predictive distribution.

Deep Ensembles. Deep Ensembles (Lakshminarayanan et al., 2017) are an ensemble method that uses DNNs as the base learners. While shallow learners aggregate ensemble predictions via majority voting, Deep Ensembles typically average the output distributions of individual members. Furthermore, individual models are generally trained independently on the same data using different random seeds for initialisation and training. Deep Ensembles are widely recognized as a way to perform approximate sampling from the posterior distribution $p(\mathbf{w} \mid \mathcal{D}) = p(\mathcal{D} \mid \mathbf{w})p(\mathbf{w})/p(\mathcal{D})$ (Wilson & Izmailov, 2020; Ashukha et al., 2020), often providing the most faithful posterior approximations (Izmailov et al., 2021). The predictive distribution of an ensemble with N members is given by

$$p(y \mid \mathbf{x}, \mathcal{D}) = \int_{\mathcal{W}} p(y \mid \mathbf{x}, \mathbf{w}) p(\mathbf{w} \mid \mathcal{D}) d\mathbf{w} \approx \frac{1}{N} \sum_{n=1}^N p(y \mid \mathbf{x}, \mathbf{w}_n), \quad (1)$$

where $\mathbf{w}_n \sim p(\mathbf{w} \mid \mathcal{D})$. Thus, it is an approximation of the posterior predictive distribution. The prediction of the Deep Ensemble, equivalent to a single model, is given by $\hat{y} = \operatorname{argmax} p(y \mid \mathbf{x}, \mathcal{D})$.

Group Fairness. Group fairness desiderata are based on the statistical dependencies between the random variables of the predicted outcomes \hat{Y} , the observed outcomes Y and the protected group attribute A . Barocas et al. (2023) define three conditions to evaluate algorithmic fairness: *independence* ($\hat{Y} \perp A$), *separation* ($\hat{Y} \perp A \mid Y$), and *sufficiency* ($Y \perp A \mid \hat{Y}$). Following widespread convention, we consider binary outcomes and protected groups, with $\hat{Y} = Y = 1$ to be the positive outcome and $A = 1$ to be the advantaged group. We measure three different notions of fairness that are common in the literature (Mehrabi et al., 2021; Caton & Haas, 2023).

First, *statistical parity* (Dwork et al., 2012; Kamishima et al., 2012), according to which fairness is achieved when the positive outcome is predicted independently of the protected group attribute. Statistical parity is also known as demographic parity. It is formally defined as

$$P(\hat{Y} = 1 \mid A = 1) = P(\hat{Y} = 1 \mid A = 0). \quad (2)$$

Second, *equal opportunity* (Hardt et al., 2016), which defines fairness as predicting the positive outcome independently of the protected group attribute, but conditioned on the observed outcome being positive. Equal opportunity is therefore formally defined as

$$P(\hat{Y} = 1 \mid A = 1, Y = 1) = P(\hat{Y} = 1 \mid A = 0, Y = 1). \quad (3)$$

Third, *equalized odds* (Hardt et al., 2016), which is a stricter version of equal opportunity where the predictive independence must hold conditioned on both positive and negative observed outcomes. Equalized odds is thus formally defined as

$$P(\hat{Y} = 1 \mid A = 1, Y = y) = P(\hat{Y} = 1 \mid A = 0, Y = y), \quad y \in \{0, 1\}. \quad (4)$$

All operationalized notions of fairness have limitations such that it is not necessarily guaranteed that changing the model predictions to satisfy the conditions given by Eq. (2) - (4) will actually lead to perfectly fair outcomes in the real world (Selbst et al., 2019; Liu et al., 2018). Furthermore, some notions of fairness can be incompatible with each other, such as statistical parity and equalized odds if A and Y are not independent (Chouldechova, 2017; Kleinberg et al., 2017). However, these metrics are still a meaningful and widely used tool to quantify group fairness.

4 Experimental Setup

Datasets. In our experiments, we evaluated Deep Ensembles on three different vision datasets. First, two facial analysis datasets, namely FairFace (Karkkainen & Joo, 2021) and UTKFace (Zhang et al., 2017). For those datasets, all models were trained on the training split of FairFace and evaluated on the official test split of FairFace and the full UTKFace dataset. Protected group attributes were binarized, except for gender which was already binary. For the attribute age, we defined young and old, where a person is considered old from 40 onwards to obtain a roughly balanced age distribution. For the attribute race, we binarized it into white vs non-white. We trained the models using one of the attributes as target variable and evaluating it with the remaining two attributes as protected group variables for all possible combinations of target and protected group attributes. Second, the CheXpert medical imaging dataset (Irvin et al., 2019) using the recommended targets provided by Jain et al. (2021) and protected group attributes provided by Gichoya et al. (2022). The no finding target was used to train and evaluate the models. Samples without all protected group attributes have been removed. A random subset of 1/8 was split as test dataset. Protected group attributes were binarized as for the facial analysis datasets. Additional details are given in Sec. D.1 in the appendix.

Models and training. We used five different DNN architectures, namely ResNet18/34/50 (He et al., 2016), RegNet-Y 800MF (Radosavovic et al., 2020) and EfficientNetV2-S (Tan & Le, 2021) for our evaluation, due to their widespread adoption and competitive performance in vision tasks. The models that were trained on the FairFace training dataset were trained for 100 epochs using SGD with momentum of 0.9 with a batch size of 256 and learning rate of 1e-2. Furthermore, a standard combination of linear (from factor 1 to 0.1) and cosine annealing schedulers was used. The models that were trained on the CheXpert training dataset were trained for 30 epochs given that the training dataset is roughly thrice the size of FairFace, resulting in a similar number of gradient steps and similar learning rate schedule. We independently trained 10 models for 5 architectures on 4 target variables with 5 seeds. Thus, a total of 1,000 individual models were obtained for our evaluation. The results discussed in the main paper correspond to using ResNet50 as the model architecture. Additional results for other model architectures are provided in Sec. F.1 and Sec. F.2 in the appendix.

Performance Metrics. We utilized accuracy as the performance metric on the FairFace and UTKFace datasets. In the case of CheXpert, we measured performance using the AUROC as established by previous work on this dataset (Zhang et al., 2022; Zong et al., 2023).

Group Fairness Metrics. We measured group fairness using empirical estimators for the fairness desiderata given by Eq. (2) - (4). Statistical Parity Difference (SPD) estimates the violation of the condition given by Eq. (2) and it is computed as

$$\text{SPD} = \text{PR}_{A=1} - \text{PR}_{A=0}, \quad (5)$$

where $\text{PR}_{A=a}$ is the positive rate calculated on the partition of the test dataset $\mathcal{D}' = \{(x_k, y_k, a_k)\}_{k=1}^K$ with the corresponding protected group attribute a . Equal Opportunity Difference (EOD) estimates the violation of the condition given by Eq. (3) and it is expressed as

$$\text{EOD} = \text{TPR}_{A=1} - \text{TPR}_{A=0}, \quad (6)$$

where $\text{TPR}_{A=a}$ is the true positive rate, calculated for the respective group partitions of the test dataset. Average Odds Difference (AOD) (Bellamy et al., 2018) is an estimator of a relaxation of equalized odds (c.f. Eq. (4)). AOD is computed by

$$\text{AOD} = \frac{1}{2} |\text{TPR}_{A=1} - \text{TPR}_{A=0}| + \frac{1}{2} |\text{FPR}_{A=1} - \text{FPR}_{A=0}|, \quad (7)$$

where $\text{FPR}_{A=a}$ is the false positive rate, calculated for the respective group partitions of the test dataset. Due to our assumption that $A = 1$ is the advantaged group, all measures are consequently $\in [0, 1]$, where 0 is the most fair. More details on Eq. (5) - (7) are given in Sec. A in the appendix.

5 The Disparate Benefits Effect of Deep Ensembles

In this section, we study the disparate benefits effect for Deep Ensembles using the experimental setup described in Sec. 4. First, we investigate the disparate benefits effect on the FairFace (FF) test dataset. Second, we apply the same models trained on FF to the UTKFace (UTK) dataset. UTK contains similar facial images as FF but from a different source, representing a realistic setting for facial analysis under slight distribution shifts. Third, we investigate the disparate benefits effect on the CheXpert (CX) medical imaging dataset to assess whether the impact on fairness of Deep Ensembles also occurs in other domains than facial analysis. Our analysis examines two primary facets of the disparate benefits effect: (i) the relationship between the number of ensemble members and the changes in performance and fairness violations (Fig. 1); and (ii) the targets and protected group attributes where a statistically significant disparate benefits effect is observed (Tab. 1).

Facial analysis (FF). The top row of Fig. 1 shows results for FF, where models were trained on target age and evaluated under the protected group attribute gender. We find that performance increases while fairness decreases when adding ensemble members. In particular, the largest decrease in fairness occurs when the first member is added to the Deep Ensemble. Tab. 1 lists the change (Δ) in performance and fairness violations between the individual models and a Deep Ensemble of 10 members for all tasks. The performance always increases for the Deep Ensemble (positive Δ). However, fairness does not necessarily increase after ensembling. We observe a disparate benefits effect with significant changes in the fairness metrics for four out of six target / protected group combinations. It occurs primarily when individual members already exhibit substantial levels of fairness violations (gray cells in Tab. 1). The strongest disparate benefits effect (largest absolute Δ) has negative impact, thus increasing the fairness violations. However, there are also cases where the Deep Ensemble is a more fair classifier than individual models (negative Δ). Overall, our results show that Deep Ensembles can decrease fairness, necessitating mitigation strategies.

Facial analysis under a distribution shift (UTK). The middle row of Fig. 1 depicts the results on the UTK dataset, with the same target and protected group as for FF (top row). Individual ensemble members exhibit higher fairness violations than for FF, which can be explained by the distribution shift between FF and UTK. However, the magnitude and behavior of the disparate benefits effect when adding ensemble members are similar to those observed with the FF dataset. The results for all target / group combinations are listed in Tab. 1. Findings for UTK are overall similar to those reported on the FF dataset. A notable exception is that the difference in SPD with target variable race and protected group attribute age is of opposite sign and larger for UTK than for FF.

Table 1: **Disparate Benefits: Change in performance and fairness violations due to ensembling.** Significant differences (Δ) between the Deep Ensemble (*c.f.* Tab 2) and the average ensemble member (*c.f.* Tab. 3) are highlighted in bold (t-test, five runs, $p < 0.05$). Gray cells denote that fairness violations are > 0.05 for both the Deep Ensemble and the average ensemble member.

\mathcal{D}'	Target / Group	Δ Accuracy (\uparrow)	Δ SPD (\downarrow)	Δ EOD (\downarrow)	Δ AOD (\downarrow)
FF	age / gender	0.022 ± 0.001	0.022 ± 0.003	0.017 ± 0.004	0.017 ± 0.003
FF	age / race	0.022 ± 0.001	0.009 ± 0.003	0.012 ± 0.004	0.007 ± 0.003
FF	gender / age	0.014 ± 0.001	-0.001 ± 0.001	-0.007 ± 0.001	-0.004 ± 0.002
FF	gender / race	0.014 ± 0.001	-0.001 ± 0.001	0.000 ± 0.000	-0.002 ± 0.002
FF	race / age	0.015 ± 0.001	-0.004 ± 0.001	0.005 ± 0.002	-0.001 ± 0.000
FF	race / gender	0.015 ± 0.001	0.000 ± 0.002	-0.008 ± 0.006	0.002 ± 0.004
UTK	age / gender	0.015 ± 0.001	0.017 ± 0.001	0.015 ± 0.002	0.012 ± 0.001
UTK	age / race	0.015 ± 0.001	0.010 ± 0.002	0.010 ± 0.001	0.004 ± 0.002
UTK	gender / age	0.009 ± 0.001	0.001 ± 0.001	-0.006 ± 0.002	-0.003 ± 0.001
UTK	gender / race	0.009 ± 0.001	0.000 ± 0.001	0.001 ± 0.002	0.001 ± 0.001
UTK	race / age	0.021 ± 0.001	0.013 ± 0.001	0.007 ± 0.002	0.000 ± 0.001
UTK	race / gender	0.021 ± 0.001	0.003 ± 0.002	-0.002 ± 0.003	-0.002 ± 0.002
\mathcal{D}'	Group	Δ AUROC (\uparrow)	Δ SPD (\downarrow)	Δ EOD (\downarrow)	Δ AOD (\downarrow)
CX	age	0.005 ± 0.000	0.001 ± 0.000	0.008 ± 0.004	0.003 ± 0.001
CX	gender	0.005 ± 0.000	0.000 ± 0.001	0.001 ± 0.004	0.001 ± 0.002
CX	race	0.005 ± 0.000	-0.002 ± 0.001	0.000 ± 0.003	-0.001 ± 0.002

Medical imaging (CX). The bottom row of Fig. 1 shows the results on the CX dataset with age as protected group attribute. The disparate benefits effect also occurs in this task, but with a smaller magnitude, which is explained by the smaller performance gains of Deep Ensembles on this dataset. Similarly as with the facial dataset, the change in fairness after adding the first ensemble member is the most pronounced in this dataset. The complete results for all protected groups are listed in Tab. 1. For the protected group age, the disparate benefits effect occurs under all fairness measures. Moreover, there is a significant difference in SPD for the protected group race, although individual models do not have substantial SPD and vice versa for EOD.

Additional results. We investigate the influence of the model size of the individual ensemble members in Sec. F.1 in the appendix. Our results show that for tasks where the disparate benefits effect occurs, it increases with model size. Furthermore, we also analyze the disparate benefits effect under different model architectures. Results and more details are given in Sec. F.2 in the appendix, finding that the results provided in the main paper are consistent across architectures. Finally, we also show the disparate benefits effect for heterogeneous Deep Ensembles in Sec. F.3 of the appendix.

6 What is the Reason for Disparate Benefits?

In this section, we investigate the potential causes behind the disparate benefits effect. We first investigate how the per-group PR, TPR and FPR metrics change when adding ensemble members, as the considered fairness metrics (Eq. (5) - Eq. (7)) are derived from them. Although this provides insight about why the disparate benefits effect occurs, it lacks an explanation for the underlying cause. We hypothesize that the disparate benefits effect results from the predictive diversity among ensemble members. Our empirical results agree with this hypothesis, suggesting that a gap in average predictive diversity between groups is causing the disparate benefits effect. We conclude with a synthetic experiment to demonstrate the soundness of our hypothesis in a controlled setting.

Changes to predictions for increasing ensemble size. We begin by examining how the metrics PR, TPR, and FPR for each group change when ensemble members are added, since the considered fairness metrics (Eq. (5) - Eq. (7)) are based on these. Fig. 2 shows these changes for the model trained on FF with age as target variable and gender as protected group, evaluated on the FF test dataset. The results show that the increase in SPD comes from a decrease in the PR of the disadvantaged

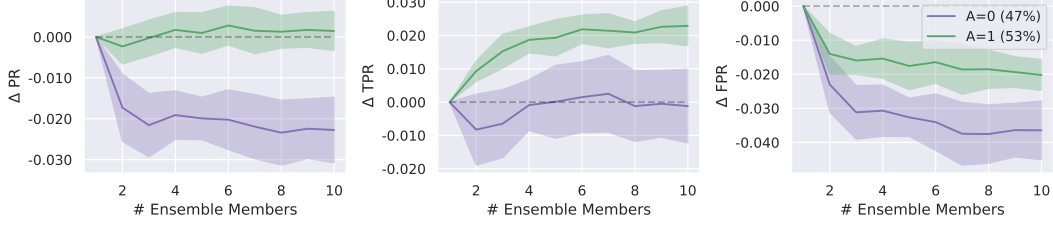


Figure 2: **Change in PR, TPR and FPR when adding members to the ensemble.** Members trained on target variable age, evaluated on the FF test dataset with gender as protected group attribute. The advantaged group $A = 1$ (male) has higher TPR and lower FPR, resulting in a net zero change in PR. The disadvantaged group $A = 0$ (female) has lower FPR and thus lower PR.

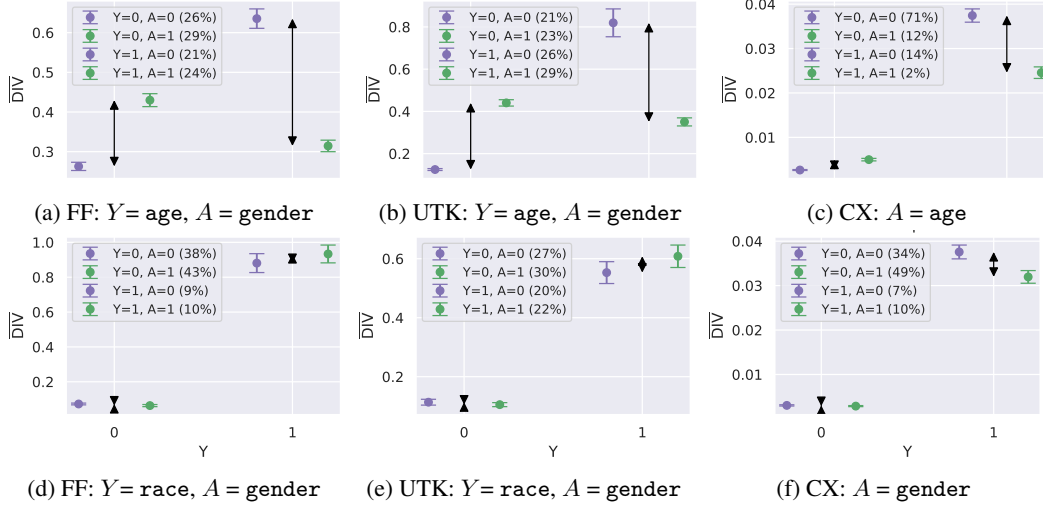


Figure 3: **Average predictive diversity ($\overline{\text{DIV}}$) per group A and target Y .** Exemplary results for datasets FF, UTK and CX. Arrows indicate per-target group differences. Top row (a)–(c): Significant disparate benefits (*c.f.* Tab. 1) occur when $\overline{\text{DIV}}$ differences between groups are large. Bottom row (d)–(f): No significant disparate benefits occur when $\overline{\text{DIV}}$ differences are small.

group when adding ensemble members, while the PR of the advantaged group remains stable. The TPR of the disadvantaged group stays constant, but the TPR of the advantaged group increases, so the Deep Ensemble improves in correctly predicting $Y = 1$ only for the advantaged group, resulting in a higher EOD. The FPR of both groups decreases, more so for the disadvantaged group, thus the Deep Ensemble improves in correctly predicting $Y = 0$ (as FPR is one minus the true negative rate). However, this doesn't offset the TPR disparity, resulting in higher AOD. Results for the remaining tasks are provided in Fig. 11 - Fig. 13 in the appendix.

Predictive diversity of ensemble members. The ensemble predictive distribution (Eq. (1)) is an average over the predictive distributions of its members. Therefore, the origin of the disparate benefits effect must be in the characteristics of the predictive distributions of individual members. Previous work investigated the predictive diversity of individual members as the driving mechanism for the increase in the performance of Deep Ensembles (Abe et al., 2022b; Jeffares et al., 2023; Abe et al., 2024). Only if individual members have different predictive distributions, combining them can lead to an ensemble that performs better than the individual models. While previous work investigates predictive diversity for individual inputs \mathbf{x} , we are interested in the average predictive diversity on the test dataset $\mathcal{D}' = \{(\mathbf{x}_k, y_k, a_k)\}_{k=1}^K$. Following from the definition of predictive diversity by Jeffares et al. (2023) (Theorem 4.3), the average predictive diversity $\overline{\text{DIV}}$ is thus given by

$$\overline{\text{DIV}} = \frac{1}{K} \sum_{k=1}^K \underbrace{\log \left(\frac{1}{N} \sum_{n=1}^N p(y = y_k | \mathbf{x}_k, \mathbf{w}_n) \right)}_{\text{Ensemble Log-Likelihood}} - \frac{1}{N} \sum_{n=1}^N \underbrace{\log p(y = y_k | \mathbf{x}_k, \mathbf{w}_n)}_{\text{Average Member Log-Likelihood}}, \quad (8)$$

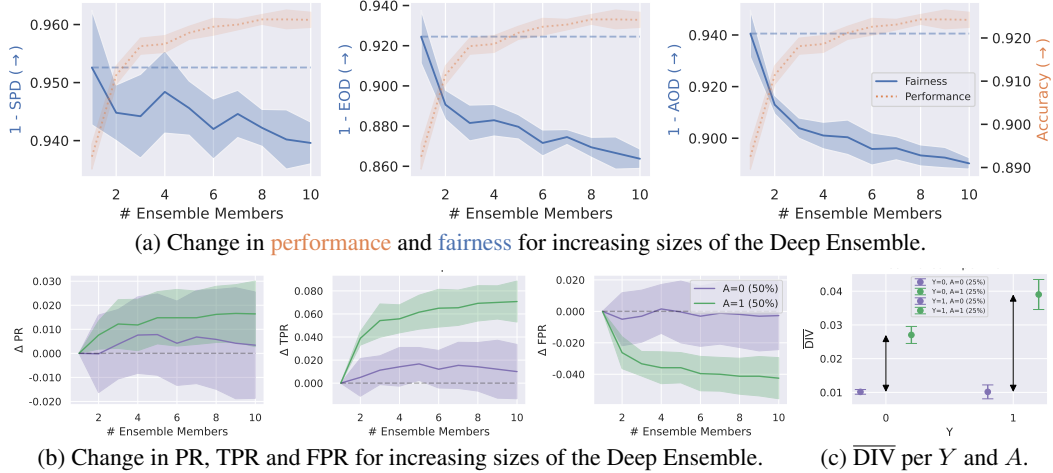


Figure 4: **Controlled experiment.** Top row: The **performance** (accuracy) increases whereas **fairness** (1-SPD, 1-EOD, 1-AOD) decreases when adding more members to the ensemble. Bottom row: The disparate benefits effect is caused by increased PR and TPR, as well as decreased FPR for the group with higher average predictive diversity $A = 1$. For the group with smaller average predictive diversity $A = 0$, there are no significant changes in PR, TPR and FPR.

for a test dataset \mathcal{D}' , and a set of N models with parameters $\{\mathbf{w}_n\}_{n=1}^N$. In Sec. C in the appendix we provide a more detailed discussion about the average predictive diversity and how it arises as a natural measure of interest from a Bayesian perspective on Deep Ensembles. In summary, the average predictive diversity estimates the ratio of the marginal likelihood of the test dataset (how well individual models agree with \mathcal{D}') and the likelihood under the Bayesian model average (how well the ensemble agrees with \mathcal{D}').

We hypothesize that differences in the average predictive diversity per group cause the disparate benefits effect. To investigate this hypothesis, we consider two sets of tasks for FF, UTK and CX, respectively: those where the disparate benefits effect occurs and those where it does not occur (*c.f.* Tab. 1). The results are depicted in Fig. 3, showing the average predictive diversity $\overline{\text{DIV}}$ per combination of the target variable Y and the protected group attribute A . In agreement with our hypothesis, tasks showing the disparate benefits effect (Fig. 3a-c) have substantial differences in average predictive diversity between groups, while tasks without the effect (Fig. 3d-f) show only minimal differences. Results on all tasks are given in Fig. 14 - Fig. 16 in the appendix.

Controlled experiment. To test our hypothesis of the per-group differences in average predictive diversity $\overline{\text{DIV}}$ causing the disparate benefits effect, we conduct a controlled experiment. We use the FashionMNIST (Xiao et al., 2017) dataset and create a binary classification problem with two targets: “T-shirt/top” ($Y = 0$) vs “Shirt” ($Y = 1$), and two groups, $A = 0$ where the same image of the same target is concatenated twice and $A = 1$ where two different images of the same target are concatenated. This is done for both the train and test datasets. An illustration of inputs \mathbf{x} for both targets and groups is given in Fig. 5. Naturally, having an input consisting of two different images ($A = 1$) should lead to more diverse ensemble members, as they may learn to use the top image, the bottom image or any combination of features from both. The combination of two identical images ($A = 0$) does not provide additional information and therefore should not lead to an increased diversity of the ensemble members. This intuition is experimentally confirmed by having a higher $\overline{\text{DIV}}$ for $A = 1$ (Fig. 4c). We observe the same behavior regarding the change in performance, fairness (Fig. 4a) as well as PR, TPR and FPR (Fig. 4b) as for the real-world datasets we investigate throughout the rest of the paper. In sum, the synthetic dataset (Fig. 5) enforces more predictive diversity for one group (Fig. 4c), leading to the disparate benefits effect (Fig. 4a, b).

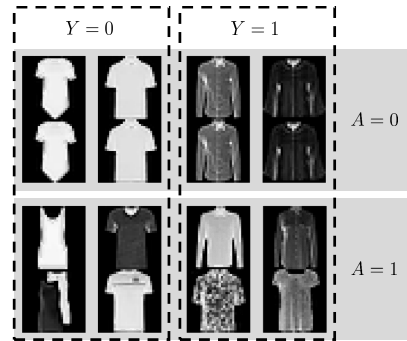


Figure 5: Inputs per target and group.

7 Mitigating the Negative Impact of Disparate Benefits

In this section, we investigate strategies to mitigate the negative consequences of the disparate benefits effect in the cases when fairness decreases due to ensembling. We focus on interventions that can be applied to trained ensemble members and thus operate in a post-processing manner. This allows to leverage the existing architecture and training procedure of the ensemble members as opposed to pre- and in-processing methods that would require expensive re-training of individual members.

First, we analyze whether it would be possible to non-uniformly weight ensemble members to attain a better trade-off between performance and fairness violations in the Deep Ensemble. Second, we examine the characteristics of the predictive distribution of the Deep Ensemble. We find that Deep Ensembles are more calibrated than individual members on our considered tasks and consequently more sensitive to the selected prediction threshold. Inspired by this finding, we investigate a group-dependent threshold optimization approach (Hardt et al., 2016), often simply referred to as Hardt post-processing (PP) in the algorithmic fairness literature, to mitigate the negative impact of the disparate benefits effect of Deep Ensembles. The results show that PP is highly effective in ensuring fairer predictions while maintaining the enhanced performance of Deep Ensembles.

Weighting of ensemble members. We analyze whether it is possible to improve the performance / fairness violations trade-off of Deep Ensembles by assigning different weights to each ensemble member, as opposed to the standard uniform weights reflected in Eq. (1). Although the results, shown in Fig. 24 in the appendix, suggest the possibility of better trade-offs, developing a method that systematically identifies the optimal weights to achieve significantly improved outcomes remains a non-trivial challenge. Specifically, we tried two approaches: selecting the best weighting on the validation set and weighting the individual ensemble members proportional to their fairness violations. Both methods lead to ensembles that are on average in between the performance and fairness violations of the Deep Ensemble with standard uniform weighting and individual models, with high variance. A detailed discussion is provided in Sec. F.4 in the appendix.

Better calibration leads to more sensitivity to the prediction threshold. Next, we analyze the predictive distribution of Deep Ensembles to identify mechanisms to mitigate the negative fairness

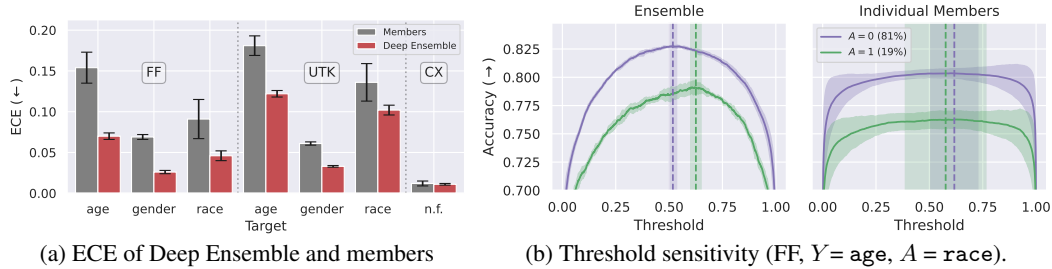


Figure 6: **Better calibration leads to more sensitivity to prediction threshold.** Deep Ensembles are more calibrated than individual members, thus have lower ECE for all considered datasets and targets (a). As a result, they are more sensitive to the selection of the prediction threshold (b).

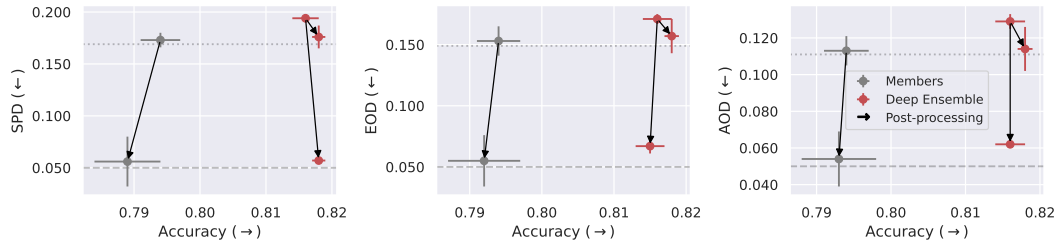


Figure 7: **Impact of applying PP on the individual members and the Deep Ensemble on FF.** Models are trained on target variable age, evaluated using protected attribute gender. Dotted lines indicate average fairness violation of individual members on the validation set, dashed line indicates 0.05 fairness violation. After PP, the Deep Ensemble maintains or improves the levels of accuracy while significantly improving its fairness, *i.e.*, has lower SPD, EOD and AOD.

consequences caused by the disparate benefits effect. Deep Ensembles are known to be better calibrated than individual models because they average over individual predictive distributions (Ovadia et al., 2019; Seligmann et al., 2023). We empirically validate this finding on our considered datasets FF, UTK and CX by evaluating the Expected Calibration Error (ECE) (Naeini et al., 2015). The results are given in Fig. 6a, showing that Deep Ensembles are indeed more calibrated (lower ECE) than individual members for all considered datasets with all possible targets Y . Being more calibrated means that the predicted probabilities correspond better to the actual outcomes. Better calibration increases the sensitivity to the prediction threshold, as even slight shifts can significantly impact predictions in a well-calibrated model (Cohen & Goldszmidt, 2004). Representative results are shown in Fig. 6b. For Deep Ensembles (Fig. 6b, left), there are clearly visible optimal values for prediction thresholds for each group (dashed lines) that are stable across multiple runs. For individual members (Fig. 6b, right), there is no clear optimal value. Any threshold between 0.2 and 0.8 leads to similar accuracies, and the optimal value is very unstable across runs. The complete results and further analysis can be found in Sec. F.5 in the appendix.

Hardt Post-Processing (PP). The sensitivity of Deep Ensembles to the selected threshold suggests that group-specific threshold optimization could be an effective unfairness mitigation strategy. A commonly used approach for this purpose in the algorithmic fairness literature is Hardt post-processing (PP) (Hardt et al., 2016). As a post-processing method, PP can be applied to the Deep Ensembles predictive distribution without changing how individual models are trained. Furthermore, PP was shown to be Pareto superior in addressing equalized odds fairness constraints compared to other fairness interventions (Cruz & Hardt, 2024), and adds minimal computational overhead.

Thus, we apply PP to the Deep Ensembles considering each of the three fairness metrics (SPD, EOD and AOD) with the aim of satisfying the fairness desiderata given in Eq. (2) - Eq. (4). Representative results for the FF dataset with age as target variable and gender as protected group attribute are depicted in Fig. 7. The complete results for all tasks are given in Tab. 4 - Tab. 18 in the appendix. As seen in Fig. 7, after applying PP, the Deep Ensembles (red dots) attain the same level of fairness violation (y-axis) as individual ensemble members (gray dots) exhibit on average, without sacrificing any performance (x-axis). This is achieved by setting the desired fairness violation for PP to the average violation of the individual members on a validation set (dotted line). In particular, the Deep Ensemble’s accuracy even increases slightly when optimizing the decision thresholds for fairness to values different from 0.5, which is the implicit threshold when using the argmax. Furthermore, we compare the Deep Ensemble and individual ensemble members after applying PP with a target fairness violation of 0.05 (dashed line). The results show that while the performance of individual members drops, the performance of the Deep Ensemble is much less affected.

8 Conclusion

In this work, we have reported on the existence of a disparate benefits effect of Deep Ensembles in experiments on three vision datasets, investigating 15 different tasks and considering five different model architectures. We have investigated potential causes for this effect, with our findings suggesting that differences in the predictive diversity of the ensemble members are a potential cause. Finally, we have evaluated different approaches to mitigate the disparate benefits effect. We find that Deep Ensembles are better calibrated than the individual members and thus more sensitive to the prediction threshold. As a result, Hardt post-processing is found to be an effective solution to ensure fairer decisions while maintaining the improved performance of Deep Ensembles.

While our experiments have focused on socially salient protected groups, we anticipate that the findings will generalize to robust classification settings where inputs can be clustered according to some group attribute. The controlled experiment provides strong evidence for this generalization.

The main limitations of our study are that we focus on vision tasks and hence on ensembles of Convolutional Neural Networks, and that we assess fairness with three group fairness metrics that, while widely used, are not sufficient to guarantee fair outcomes. The fairness of predictions of a model in the real-world can’t be reduced to any single metric and must be carefully assessed depending on the application. In future work, we thus plan to explore other notions of fairness, such as individual fairness, and extend our analysis to other types of models and datasets, including text. Furthermore, we intend to investigate the disparate benefits effect for Deep Ensembles where pre- or in-processing fairness methods have been applied to individual ensemble members.

Acknowledgements

We thank Julien Colin, Vihang Patil and Aditya Gulati for their constructive feedback on our work.

The ELLIS Unit Linz, the LIT AI Lab, the Institute for Machine Learning, are supported by the Federal State Upper Austria. We thank the projects Medical Cognitive Computing Center (MC3), INCONTROL-RL (FFG-881064), PRIMAL (FFG-873979), S3AI (FFG-872172), DL for GranularFlow (FFG-871302), EPILEPSIA (FFG-892171), AIRI FG 9-N (FWF-36284, FWF-36235), AI4GreenHeatingGrids (FFG- 899943), INTEGRATE (FFG-892418), ELISE (H2020-ICT-2019-3 ID: 951847), Stars4Waters (HORIZON-CL6-2021-CLIMATE-01-01). We thank NXAI GmbH, Audi.JKU Deep Learning Center, TGW LOGISTICS GROUP GMBH, Silicon Austria Labs (SAL), FILL Gesellschaft mbH, Anyline GmbH, Google, ZF Friedrichshafen AG, Robert Bosch GmbH, UCB Biopharma SRL, Merck Healthcare KGaA, Verbund AG, GLS (Univ. Waterloo), Software Competence Center Hagenberg GmbH, Borealis AG, TÜV Austria, Frauscher Sonsonic, TRUMPF and the NVIDIA Corporation.

The ELLIS Unit Alicante Foundation acknowledges support from by Intel corporation, a nominal grant received at the ELLIS Unit Alicante Foundation from the Regional Government of Valencia in Spain (Convenio Singular signed with Generalitat Valenciana, Conselleria de Innovación, Industria, Comercio y Turismo, Dirección General de Innovación) and a grant by the Banc Sabadell Foundation. In addition, it is funded by the European Union EU - HE ELIAS – Grant Agreement 101120237. Views and opinions expressed are however those of the author(s) only and do not necessarily reflect those of the European Union or the European Health and Digital Executive Agency (HaDEA).

Kajetan Schweighofer acknowledges travel support from ELISE (GA no 951847).

References

- Abe, T., Buchanan, E. K., Pleiss, G., and Cunningham, J. P. The best deep ensembles sacrifice predictive diversity. In *I Can't Believe It's Not Better Workshop: Understanding Deep Learning Through Empirical Falsification*, 2022a.
- Abe, T., Buchanan, E. K., Pleiss, G., Zemel, R., and Cunningham, J. P. Deep ensembles work, but are they necessary? In Koyejo, S., Mohamed, S., Agarwal, A., Belgrave, D., Cho, K., and Oh, A. (eds.), *Advances in Neural Information Processing Systems*, volume 35, pp. 33646–33660. Curran Associates, Inc., 2022b.
- Abe, T., Buchanan, E. K., Pleiss, G., and Cunningham, J. P. Pathologies of predictive diversity in deep ensembles. *Transactions on Machine Learning Research*, 2024.
- Agarwal, A., Beygelzimer, A., Dudík, M., Langford, J., and Wallach, H. A reductions approach to fair classification. In *International conference on machine learning*, pp. 60–69. PMLR, 2018.
- Arnaiz-Rodriguez, A. and Oliver, N. Towards algorithmic fairness by means of instance-level data re-weighting based on shapley values. In *ICLR 2024 Workshop on Data-centric Machine Learning Research (DMLR)*, 2024.
- Ashukha, A., Lyzhov, A., Molchanov, D., and Vetrov, D. Pitfalls of in-domain uncertainty estimation and ensembling in deep learning. In *International Conference on Learning Representations*, 2020.
- Barocas, S. and Selbst, A. D. Big data's disparate impact. *Calif. L. Rev.*, 104:671, 2016.
- Barocas, S., Hardt, M., and Narayanan, A. *Fairness and Machine Learning: Limitations and Opportunities*. MIT Press, 2023.
- Bellamy, R. K. E., Dey, K., Hind, M., Hoffman, S. C., Houde, S., Kannan, K., Lohia, P., Martino, J., Mehta, S., Mojsilovic, A., Nagar, S., Ramamurthy, K. N., Richards, J., Saha, D., Sattigeri, P., Singh, M., Varshney, K. R., and Zhang, Y. Ai fairness 360: An extensible toolkit for detecting, understanding, and mitigating unwanted algorithmic bias. *arXiv*, 1810.01943, 2018.
- Bhusal, N., Shukla, R. M., Gautam, M., Benidris, M., and Sengupta, S. Deep ensemble learning-based approach to real-time power system state estimation. *International Journal of Electrical Power & Energy Systems*, 129:106806, 2021.

- Binns, R. Fairness in machine learning: Lessons from political philosophy. In *Conference on fairness, accountability and transparency*, pp. 149–159. PMLR, 2018.
- Black, E., Leino, K., and Fredrikson, M. Selective ensembles for consistent predictions. In *International Conference on Learning Representations*, 2022a.
- Black, E., Raghavan, M., and Barocas, S. Model multiplicity: Opportunities, concerns, and solutions. In *Proceedings of the 2022 ACM Conference on Fairness, Accountability, and Transparency*, FAccT ’22, pp. 850–863, New York, NY, USA, 2022b. Association for Computing Machinery.
- Carey, A. N. and Wu, X. The statistical fairness field guide: perspectives from social and formal sciences. *AI and Ethics*, 3(1):1–23, 2023.
- Caton, S. and Haas, C. Fairness in machine learning: A survey. *ACM Comput. Surv.*, aug 2023.
- Chouldechova, A. Fair prediction with disparate impact: A study of bias in recidivism prediction instruments. *Big data*, 5(2):153–163, 2017.
- Cohen, I. and Goldszmidt, M. Properties and benefits of calibrated classifiers. In *European conference on principles of data mining and knowledge discovery*, pp. 125–136. Springer, 2004.
- Cooper, A. F., Lee, K., Choksi, M. Z., Barocas, S., De Sa, C., Grimmelmann, J., Kleinberg, J., Sen, S., and Zhang, B. Arbitrariness and social prediction: The confounding role of variance in fair classification. *Proceedings of the AAAI Conference on Artificial Intelligence*, 38(20):22004–22012, 03 2024.
- Corbett-Davies, S., Pierson, E., Feller, A., Goel, S., and Huq, A. Algorithmic decision making and the cost of fairness. In *Proceedings of the 23rd acm sigkdd international conference on knowledge discovery and data mining*, pp. 797–806, 2017.
- Coston, A., Rambachan, A., and Chouldechova, A. Characterizing fairness over the set of good models under selective labels. In Meila, M. and Zhang, T. (eds.), *Proceedings of the 38th International Conference on Machine Learning*, volume 139 of *Proceedings of Machine Learning Research*, pp. 2144–2155. PMLR, 18–24 Jul 2021.
- Cruz, A. and Hardt, M. Unprocessing seven years of algorithmic fairness. In *The Twelfth International Conference on Learning Representations*, 2024.
- Dolezal, J. M., Srisuwananukorn, A., Karpeyev, D., Ramesh, S., Kochanny, S., Cody, B., Mansfield, A. S., Rakshit, S., Bansal, R., Bois, M. C., Bungum, A. O., Schulte, J. J., Vokes, E. E., Garassino, M. C., Husain, A. N., and Pearson, A. T. Uncertainty-informed deep learning models enable high-confidence predictions for digital histopathology. *Nature Communications*, 13(1):6572, Nov 2022.
- Dwork, C., Hardt, M., Pitassi, T., Reingold, O., and Zemel, R. Fairness through awareness. In *Proceedings of the 3rd Innovations in Theoretical Computer Science Conference*, ITCS ’12, pp. 214–226, New York, NY, USA, 2012. Association for Computing Machinery.
- Fort, S., Hu, H., and Lakshminarayanan, B. Deep ensembles: A loss landscape perspective. *arXiv*, 1912.02757, 2019.
- Garg, P., Villasenor, J., and Foggo, V. Fairness metrics: A comparative analysis. In *2020 IEEE international conference on big data (Big Data)*, pp. 3662–3666. IEEE, 2020.
- Gichoya, J. W., Banerjee, I., Bhimireddy, A. R., Burns, J. L., Celi, L. A., Chen, L.-C., Correa, R., Dullerud, N., Ghassemi, M., Huang, S.-C., Kuo, P.-C., Lungren, M. P., Palmer, L. J., Price, B. J., Purkayastha, S., Pyrros, A. T., Oakden-Rayner, L., Okechukwu, C., Seyyed-Kalantari, L., Trivedi, H., Wang, R., Zaiman, Z., and Zhang, H. Ai recognition of patient race in medical imaging: a modelling study. *The Lancet Digital Health*, 4(6):e406–e414, June 2022.
- Hardt, M., Price, E., Price, E., and Srebro, N. Equality of opportunity in supervised learning. In Lee, D., Sugiyama, M., Luxburg, U., Guyon, I., and Garnett, R. (eds.), *Advances in Neural Information Processing Systems*, volume 29. Curran Associates, Inc., 2016.

- He, K., Zhang, X., Ren, S., and Sun, J. Deep residual learning for image recognition. In *2016 IEEE Conference on Computer Vision and Pattern Recognition (CVPR)*, pp. 770–778, 2016.
- Irvin, J., Rajpurkar, P., Ko, M., Yu, Y., Ciurea-Ilcus, S., Chute, C., Marklund, H., Haghighi, B., Ball, R., Shpanskaya, K., Seekins, J., Mong, D. A., Halabi, S. S., Sandberg, J. K., Jones, R., Larson, D. B., Langlotz, C. P., Patel, B. N., Lungren, M. P., and Ng, A. Y. Chexpert: A large chest radiograph dataset with uncertainty labels and expert comparison. *Proceedings of the AAAI Conference on Artificial Intelligence*, 33:590–597, Jul. 2019.
- Izmailov, P., Vikram, S., Hoffman, M. D., and Wilson, A. G. G. What are bayesian neural network posteriors really like? In Meila, M. and Zhang, T. (eds.), *Proceedings of the 38th International Conference on Machine Learning*, volume 139 of *Proceedings of Machine Learning Research*, pp. 4629–4640. PMLR, 18–24 Jul 2021.
- Jain, S., Smit, A., Truong, S. Q., Nguyen, C. D., Huynh, M.-T., Jain, M., Young, V. A., Ng, A. Y., Lungren, M. P., and Rajpurkar, P. Visualchexpert: addressing the discrepancy between radiology report labels and image labels. In *Proceedings of the Conference on Health, Inference, and Learning*, pp. 105–115. Association for Computing Machinery, 2021.
- Jeffares, A., Liu, T., Crabbé, J., and van der Schaar, M. Joint training of deep ensembles fails due to learner collusion. In Oh, A., Neumann, T., Globerson, A., Saenko, K., Hardt, M., and Levine, S. (eds.), *Advances in Neural Information Processing Systems*, volume 36, pp. 13559–13589. Curran Associates, Inc., 2023.
- Jung, S., Park, T., Chun, S., and Moon, T. Re-weighting based group fairness regularization via class-wise robust optimization. In *The Eleventh International Conference on Learning Representations*, 2023.
- Kamiran, F. and Calders, T. Data preprocessing techniques for classification without discrimination. *Knowledge and information systems*, 33(1):1–33, 2012.
- Kamishima, T., Akaho, S., Asoh, H., and Sakuma, J. Fairness-aware classifier with prejudice remover regularizer. In Flach, P. A., De Bie, T., and Cristianini, N. (eds.), *Machine Learning and Knowledge Discovery in Databases*, pp. 35–50, Berlin, Heidelberg, 2012. Springer Berlin Heidelberg.
- Karkkainen, K. and Joo, J. Fairface: Face attribute dataset for balanced race, gender, and age for bias measurement and mitigation. In *Proceedings of the IEEE/CVF Winter Conference on Applications of Computer Vision*, pp. 1548–1558, 2021.
- Kleinberg, J., Mullainathan, S., and Raghavan, M. Inherent trade-offs in the fair determination of risk scores. In *8th Innovations in Theoretical Computer Science*, 2017.
- Ko, W.-Y., D’souza, D., Nguyen, K., Balestrieri, R., and Hooker, S. Fair-ensemble: When fairness naturally emerges from deep ensembling. *arXiv*, 2303.00586, 2023.
- Kusner, M. J., Loftus, J., Russell, C., and Silva, R. Counterfactual fairness. *Advances in neural information processing systems*, 30, 2017.
- Lakshminarayanan, B., Pritzel, A., and Blundell, C. Simple and scalable predictive uncertainty estimation using deep ensembles. In Guyon, I., Luxburg, U. V., Bengio, S., Wallach, H., Fergus, R., Vishwanathan, S., and Garnett, R. (eds.), *Advances in Neural Information Processing Systems*, volume 30. Curran Associates, Inc., 2017.
- Lanitis, A., Taylor, C., and Cootes, T. Toward automatic simulation of aging effects on face images. *IEEE Transactions on Pattern Analysis and Machine Intelligence*, 24(4):442–455, 2002.
- Lee, Y., Yao, H., and Finn, C. Diversify and disambiguate: Out-of-distribution robustness via disagreement. In *The Eleventh International Conference on Learning Representations*, 2023.
- Liu, L. T., Dean, S., Rolf, E., Simchowitz, M., and Hardt, M. Delayed impact of fair machine learning. In *International Conference on Machine Learning*, pp. 3150–3158. PMLR, 2018.
- Long, C. X., Hsu, H., Alghamdi, W., and Calmon, F. P. Arbitrariness lies beyond the fairness-accuracy frontier. *arXiv*, 2306.09425, 2023.

- Marx, C., Calmon, F., and Ustun, B. Predictive multiplicity in classification. In III, H. D. and Singh, A. (eds.), *Proceedings of the 37th International Conference on Machine Learning*, volume 119 of *Proceedings of Machine Learning Research*, pp. 6765–6774. PMLR, 13–18 Jul 2020.
- Mehrabi, N., Morstatter, F., Saxena, N., Lerman, K., and Galstyan, A. A survey on bias and fairness in machine learning. *ACM Comput. Surv.*, 54(6), jul 2021.
- Naeini, M. P., Cooper, G., and Hauskrecht, M. Obtaining well calibrated probabilities using bayesian binning. In *Proceedings of the AAAI conference on artificial intelligence*, volume 29, 2015.
- Ovadia, Y., Fertig, E., Ren, J., Nado, Z., Sculley, D., Nowozin, S., Dillon, J., Lakshminarayanan, B., and Snoek, J. Can you trust your model's uncertainty? evaluating predictive uncertainty under dataset shift. In Wallach, H., Larochelle, H., Beygelzimer, A., d'Alché-Buc, F., Fox, E., and Garnett, R. (eds.), *Advances in Neural Information Processing Systems*, volume 32. Curran Associates, Inc., 2019.
- Pagliardini, M., Jaggi, M., Fleuret, F., and Karimireddy, S. P. Agree to disagree: Diversity through disagreement for better transferability. In *The Eleventh International Conference on Learning Representations*, 2023.
- Paszke, A., Gross, S., Massa, F., Lerer, A., Bradbury, J., Chanan, G., Killeen, T., Lin, Z., Gimelshein, N., Antiga, L., Desmaison, A., Kopf, A., Yang, E., DeVito, Z., Raison, M., Tejani, A., Chilamkurthy, S., Steiner, B., Fang, L., Bai, J., and Chintala, S. Pytorch: An imperative style, high-performance deep learning library. *Advances in Neural Information Processing Systems*, 32, 2019.
- Pombal, J., Cruz, A. F., Bravo, J., Saleiro, P., Figueiredo, M. A. T., and Bizarro, P. Understanding unfairness in fraud detection through model and data bias interactions. *arXiv*, 2207.06273, 2022.
- Radosavovic, I., Kosaraju, R. P., Girshick, R., He, K., and Dollar, P. Designing network design spaces. In *Proceedings of the IEEE/CVF Conference on Computer Vision and Pattern Recognition (CVPR)*, June 2020.
- Rame, A. and Cord, M. DICE: Diversity in deep ensembles via conditional redundancy adversarial estimation. In *International Conference on Learning Representations*, 2021.
- Sagawa, S., Koh, P. W., Hashimoto, T. B., and Liang, P. Distributionally robust neural networks. In *International Conference on Learning Representations*, 2020.
- Schweighofer, K., Aichberger, L., Ielanskyi, M., Klambauer, G., and Hochreiter, S. Quantification of uncertainty with adversarial models. In Oh, A., Naumann, T., Globerson, A., Saenko, K., Hardt, M., and Levine, S. (eds.), *Advances in Neural Information Processing Systems*, volume 36, pp. 19446–19484. Curran Associates, Inc., 2023.
- Selbst, A. D., Boyd, D., Friedler, S. A., Venkatasubramanian, S., and Vertesi, J. Fairness and abstraction in sociotechnical systems. In *Proceedings of the conference on fairness, accountability, and transparency*, pp. 59–68, 2019.
- Seligmann, F., Becker, P., Volpp, M., and Neumann, G. Beyond deep ensembles: A large-scale evaluation of bayesian deep learning under distribution shift. In Oh, A., Naumann, T., Globerson, A., Saenko, K., Hardt, M., and Levine, S. (eds.), *Advances in Neural Information Processing Systems*, volume 36, pp. 29372–29405. Curran Associates, Inc., 2023.
- Tan, M. and Le, Q. Efficientnetv2: Smaller models and faster training. In Meila, M. and Zhang, T. (eds.), *Proceedings of the 38th International Conference on Machine Learning*, volume 139 of *Proceedings of Machine Learning Research*, pp. 10096–10106. PMLR, 18–24 Jul 2021.
- Wilson, A. G. and Izmailov, P. Bayesian deep learning and a probabilistic perspective of generalization. In Larochelle, H., Ranzato, M., Hadsell, R., Balcan, M., and Lin, H. (eds.), *Advances in Neural Information Processing Systems*, volume 33, pp. 4697–4708. Curran Associates, Inc., 2020.
- Xia, L., Chen, C., and Aggarwal, J. View invariant human action recognition using histograms of 3d joints. In *Computer Vision and Pattern Recognition Workshops (CVPRW), 2012 IEEE Computer Society Conference on*, pp. 20–27. IEEE, 2012.

- Xiao, H., Rasul, K., and Vollgraf, R. Fashion-mnist: a novel image dataset for benchmarking machine learning algorithms. *arXiv*, 1708.07747, 2017.
- Zafar, M. B., Valera, I., Gomez Rodriguez, M., and Gummadi, K. P. Fairness Beyond Disparate Treatment & Disparate Impact: Learning Classification without Disparate Mistreatment. In *International Conference on World Wide Web*, pp. 1171–1180, 2017.
- Zhang, B. H., Lemoine, B., and Mitchell, M. Mitigating unwanted biases with adversarial learning. In *AIES '18*, pp. 335–340, New York, NY, USA, 2018. Association for Computing Machinery.
- Zhang, H., Dullerud, N., Roth, K., Oakden-Rayner, L., Pfohl, S., and Ghassemi, M. Improving the fairness of chest x-ray classifiers. In Flores, G., Chen, G. H., Pollard, T., Ho, J. C., and Naumann, T. (eds.), *Proceedings of the Conference on Health, Inference, and Learning*, volume 174 of *Proceedings of Machine Learning Research*, pp. 204–233. PMLR, 07-08 Apr 2022.
- Zhang, Z., Song, Y., and Qi, H. Age progression/regression by conditional adversarial autoencoder. In *IEEE Conference on Computer Vision and Pattern Recognition (CVPR)*. IEEE, 2017.
- Zong, Y., Yang, Y., and Hospedales, T. MEDFAIR: Benchmarking fairness for medical imaging. In *The Eleventh International Conference on Learning Representations*, 2023.

A Details on Computing Group Fairness Metrics

Group fairness metrics, as previously discussed, are based on assumptions related to the independence of the prediction with respect to the protected attribute and the target. For completeness, we present below how to estimate the metrics given in Eq. (5) - Eq. (7) with samples. We start by defining the number of correct (TP, TN) and wrong decisions (FP, FN) of a model:

$$\begin{aligned} \text{TP} &:= \sum_{k=1}^K \mathbb{1}[f(\mathbf{x}_k) > t] \mathbb{1}[y_k = 1], & \text{TN} &:= \sum_{k=1}^K \mathbb{1}[f(\mathbf{x}_k) < t] \mathbb{1}[y_k = 0] \\ \text{FP} &:= \sum_{k=1}^K \mathbb{1}[f(\mathbf{x}_k) > t] \mathbb{1}[y_k = 0], & \text{FN} &:= \sum_{k=1}^K \mathbb{1}[f(\mathbf{x}_k) < t] \mathbb{1}[y_k = 1]. \end{aligned}$$

Here, $\mathcal{D}' = \{(\mathbf{x}_k, y_k, a_k)\}_{k=1}^K$ is the test dataset; a datapoint (\mathbf{x}_k, y_k, a_k) consists of input features, observed outcome and protected group attribute; $f(\mathbf{x}_k)$ is the model's predicted value for \mathbf{x}_k ; and t is the classification threshold. To compute these metrics for a specific value a of protected group attribute A (e.g., male for gender), we add the term $\mathbb{1}[a_k = a]$ to each computation, resulting in group-specific true positives $\text{TP}_{A=a}$, true negatives $\text{TN}_{A=a}$, false positives $\text{FP}_{A=a}$, and false negatives $\text{FN}_{A=a}$.

Once all these buliding blocks are computed, the group-specific Positive Rate ($\text{PR}_{A=a}$) is given by

$$\text{PR}_{A=a} = P(\hat{Y} = 1 \mid A = a) \approx \frac{\text{TP}_{A=a} + \text{FP}_{A=a}}{\text{TP}_{A=a} + \text{FP}_{A=a} + \text{TN}_{A=a} + \text{FN}_{A=a}}.$$

Finally, equal opportunity and equalized odds depend on the *conditional* true/false negative/positive rates, depending on the values of the protected group attribute A and are calculated as:

$$\begin{aligned} \text{TPR}_{A=a} &= P(\hat{Y} = 1 \mid Y = 1, A = a) \approx \frac{\text{TP}_{A=a}}{\text{TP}_{A=a} + \text{FN}_{A=a}} \\ \text{TNR}_{A=a} &= P(\hat{Y} = 0 \mid Y = 0, A = a) \approx \frac{\text{TN}_{A=a}}{\text{FP}_{A=a} + \text{TN}_{A=a}} \\ \text{FPR}_{A=a} &= P(\hat{Y} = 1 \mid Y = 0, A = a) \approx \frac{\text{FP}_{A=a}}{\text{FP}_{A=a} + \text{TN}_{A=a}} \\ \text{FNR}_{A=a} &= P(\hat{Y} = 0 \mid Y = 1, A = a) \approx \frac{\text{FN}_{A=a}}{\text{TP}_{A=a} + \text{FN}_{A=a}} \end{aligned}$$

A.1 Group fairness metrics as a factorization of $P(Y, \hat{Y} \mid A)$.

In order to analyze the trade-offs and connections between different statistical group fairness metrics, a common approach is to use the factorization of $P(Y, \hat{Y} \mid A)$, which offers a clear intuition of the incompatibilities between some of them. Then, all the introduced metrics are related as per:

$$\begin{aligned} P(\hat{Y} \mid Y, A = 1) \times P(Y \mid A = 1) &= P(Y \mid \hat{Y}, A = 1) \times P(\hat{Y} \mid A = 1) \\ \underbrace{P(\hat{Y} \mid Y, A = 0)}_{\substack{\text{Separation} \\ \hat{Y} \perp A \mid Y \\ \text{e.g. AOD, EOD}}} \times \underbrace{P(Y \mid A = 0)}_{\substack{\text{Prevalence Eq.} \\ Y \perp A}} &= \underbrace{P(Y \mid \hat{Y}, A = 0)}_{\substack{\text{Sufficiency} \\ Y \perp A \mid \hat{Y}}} \times \underbrace{P(\hat{Y} \mid A = 0)}_{\substack{\text{Independence} \\ \hat{Y} \perp A \\ \text{e.g. SPD}}} \end{aligned} \quad (9)$$

For instance, it suggests that, if the target prevalence is different across groups and the model is perfectly calibrated (sufficiency), then separation and independence conditions cannot be satisfied simultaneously.

B Biases and Group Unfairness

Biases induced by datasets have been studied in [Pombal et al. \(2022\)](#). They consider the joint distribution $P(X, Y, A)$. Generally there is a bias under a distribution shift with $P^*(X, Y, A) \neq P(X, Y, A)$, where the distribution after the shift P^* the model is applied on is different to the

distribution P the training data was sampled from. Furthermore, Pombal et al. (2022) consider biases in the training data distribution. A bias arises if

$$P(X, Y) \neq P(X, Y | A), \quad (10)$$

as well as if $P(A)$ is not a uniform distribution. Note that $P(X, Y | A)$ can be factorized into

$$\begin{aligned} P(X, Y | A) &= P(X | Y, A) P(X | A) \\ &= P(Y | X, A) P(Y | A). \end{aligned} \quad (11)$$

Different parts of the factorization in Eq. (11) can lead to unfairness:

- $P(Y) \neq P(Y | A)$ corresponds to a *prevalence disparity*, i.e., the class probability depends on the protected attribute. This imbalance is not present in FairFace dataset since it has been specifically curated to avoid this problem (Karkkainen & Joo, 2021). However, we observe it in the UTKFace and CheXpert datasets.
- $P(X | Y) \neq P(X | Y, A)$ reflects a *group-wise disparity of the class-conditional distribution*, and indicates that the feature space is distributed differently depending on the protected attribute, which is undesirable, since the likelihood of $p(\mathcal{D} | \mathbf{w})$ could vary across protected groups, leading to potentially different per-group error rates and hence unfairness. The experimental results in Fig. (3) illustrate differences in the likelihood of the dataset for different (A, Y) .
- $P(Y | X) \neq P(Y | X, A)$ represents *noisy targets*. In this case, the distribution of Y given X depends on the protected group attribute. The classification experiments in Tab. 1, Fig. 1 and Fig. 2 analyze metrics related to $P(Y | X, A)$ and the resulting accuracy and fairness violations.

C Bayesian Perspective on the Average Predictive Diversity

In this section, we motivate the average predictive diversity $\overline{\text{DIV}}$ (c.f. Eq. (8)) from a Bayesian perspective. Given are a training dataset $\mathcal{D} = \{(\mathbf{x}_j, y_j)\}_{j=1}^J$ as well as a test dataset $\mathcal{D}' = \{(\mathbf{x}_k, y_k)\}_{k=1}^K$; the protected attribute is omitted for brevity in this section. Furthermore, we are given a prior distribution $p(\mathbf{w})$ on the model parameters.

Marginal Likelihood. Through Bayes' rule, we obtain a posterior distribution over the model parameters given the training dataset $p(\mathbf{w} | \mathcal{D}) = p(\mathcal{D} | \mathbf{w})p(\mathbf{w})/p(\mathcal{D})$. Recall that the marginal likelihood is given by $p(\mathcal{D}) = \int_W p(\mathcal{D} | \mathbf{w})p(\mathbf{w})d\mathbf{w}$, i.e., the expected likelihood on the dataset over all models according to their prior distribution. Intuitively, the marginal likelihood thus measures how well possible models represent the given dataset.

The disparate benefits effect occurs on a test dataset \mathcal{D}' . Consequently, we are interested in the marginal likelihood under the test dataset $p(\mathcal{D}')$. For the test dataset \mathcal{D}' , the posterior distribution given the training dataset $p(\mathbf{w} | \mathcal{D})$ is the new prior distribution $p(\mathbf{w})$. The marginal likelihood under the test dataset is thus given by

$$p(\mathcal{D}') = \int_W \prod_{k=1}^K p(y = y_k | \mathbf{x}_k, \mathbf{w}) p(\mathbf{w}) d\mathbf{w} \approx \frac{1}{N} \sum_{n=1}^N \prod_{k=1}^K p(y = y_k | \mathbf{x}_k, \mathbf{w}_n), \quad (12)$$

with \mathbf{w}_n drawn according to $p(\mathbf{w}) = p(\mathbf{w} | \mathcal{D})$. In practice, the set of model parameters $\{\mathbf{w}_n\}_{n=1}^N$ obtained from the training of the Deep Ensemble is used to approximate the integral.

Likelihood Ratio. If the likelihood under the posterior predictive distribution

$$\bar{p}(\mathcal{D}') = \prod_{k=1}^K \int_W p(y = y_k | \mathbf{x}_k, \mathbf{w}) p(\mathbf{w} | \mathcal{D}) d\mathbf{w} \approx \prod_{k=1}^K \frac{1}{N} \sum_{n=1}^N p(y = y_k | \mathbf{x}_k, \mathbf{w}_n), \quad (13)$$

again with \mathbf{w}_n drawn according to $p(\mathbf{w}) = p(\mathbf{w} | \mathcal{D})$, does not differ from the marginal likelihood, there is no difference between predicting with a single model sampled according to the posterior and predicting with the ensemble of all sampled models. Thus, we investigate the likelihood ratio $\bar{p}(\mathcal{D}')/p(\mathcal{D}')$ as a natural measure of diversity in the predictions of the models that make up the ensemble.

For practical purposes, it is more convenient to work with log-likelihoods rather than likelihoods, as the products in Eq. (13) and Eq. (13) become sums. Therefore, we consider the logarithm of the likelihood ratio, leading to

$$\log \left(\frac{\bar{p}(\mathcal{D}')}{p(\mathcal{D}')} \right) = \log \bar{p}(\mathcal{D}') - \log p(\mathcal{D}'). \quad (14)$$

Inserting Eq. (12) and Eq. (13) into Eq. (14) we obtain

$$\begin{aligned} \log \left(\frac{\bar{p}(\mathcal{D}')}{p(\mathcal{D}')} \right) &\approx \sum_{k=1}^K \log \left(\frac{1}{N} \sum_{n=1}^N p(y = y_k | \mathbf{x}_k, \mathbf{w}_n) \right) - \frac{1}{N} \sum_{n=1}^N \log p(y = y_k | \mathbf{x}_k, \mathbf{w}_n) \\ &= K \overline{\text{DIV}}, \end{aligned} \quad (15)$$

with $\overline{\text{DIV}}$ as defined in Eq. (8), which is what we wanted to show. Eq. (15) is $\sum_{k=1}^K \text{DIV}$, with the predictive diversity DIV given by Theorem 4.3 in Jeffares et al. (2023). To mitigate the impact of different dataset sizes, it is common practice to divide log-likelihoods by the number of datapoints in the dataset K when comparing between datasets of different sizes. Doing so for the logarithm of the likelihood ratio, $1/K \log (\bar{p}(\mathcal{D}')/p(\mathcal{D}'))$ is an approximation of the Jensen gap (Eq. (5) in Abe et al. (2022a) and Eq. (3) in Abe et al. (2024)) with K samples in the dataset \mathcal{D}' .

D Details of the Experimental Setup

The code to reproduce our experiments is available at <https://github.com/ml-jku/disparate-benefits>.

D.1 Datasets

We conducted all our experiments on facial analysis and medical imaging datasets. In the following, we provide details about the datasets.

Facial Analysis. We used two widely used facial analysis datasets, FairFace¹ (Karkkainen & Joo, 2021) (License: CC BY 4.0) and UTKFace² (Zhang et al., 2017) (License: research only, not commercial). FairFace was created for advancing research in fairness, accountability and transparency in computer vision as it addresses the lack of diversity in existing face datasets used for research purposes. The FairFace dataset comprises 108,501 facial images collected from publicly available sources, such as Flickr and Google Images, and covers a diverse range of demographics, including various ethnicities, ages, genders, and skin tones. The dataset includes annotations for gender, age, and ethnicity. UTKFace contains over 20,000 facial images of individuals collected from the publicly available datasets UTKinect (Xia et al., 2012) and FGNET (Lanitis et al., 2002), as well as images scraped from the internet. It includes annotations for three demographic attributes: age, gender, and ethnicity.

Medical Imaging. We used the medical imaging dataset CheXpert³ (Irvin et al., 2019) (License: Stanford University Dataset Research Use Agreement). It consists of a large publicly available dataset of 224,316 chest X-rays along with associated radiologist-labeled annotations for the presence or absence of 14 different thoracic pathologies. It is designed to address the challenges of class imbalance and target noise commonly encountered in medical image classification tasks. CheXpert has become a widely used benchmark dataset in the field of medical imaging and has been instrumental in advancing research on automated chest radiograph interpretation, particularly in the context of deep learning approaches. We use the recommended targets provided by Jain et al. (2021) (visualCheXbert targets) and group attributes provided by Gichoya et al. (2022)⁴.

¹Obtained from <https://github.com/joojs/fairface> using the [Padding=0.25] version.

²Obtained from <https://www.kaggle.com/datasets/abhikjha/utk-face-cropped> as the download link on the original source <https://susanqq.github.io/UTKFace> does no longer work.

³Obtained from <https://stanfordaimi.azurewebsites.net/datasets/8cbd9ed4-2eb9-4565-affc-111cf4f7ebe2>, user account required.

⁴Obtained from <https://stanfordaimi.azurewebsites.net/datasets/192ada7c-4d43-466e-b8bb-b81992bb80cf>, user account required.

D.2 Models and Training

We used the ResNet18/24/50, RegNet-Y 800MF and EfficientNetV2-S implementations of Pytorch (Paszke et al., 2019). Hyperparameters as reported in the main paper were the result of an initial manual tuning on the respective validation sets, but mostly align with commonly utilized hyperparameters for classical image datasets such as CIFAR10. The raw performance on the task was not of extreme importance, but is comparable to previous studies on the same datasets with similar network architectures (Karkkainen & Joo, 2021; Zhang et al., 2022; Zong et al., 2023).

D.3 Computational Cost

For training the models, we utilized a mixture of P100, RTX 3090, A40 and A100 GPUs, depending on availability in our cluster. Training a single model took around 3 hours on average over all considered model architectures and datasets, resulting in 3,000 GPU-hours. Evaluating these models on the test datasets accounted for approximately 150 additional GPU-hours.

E Complete Experimental Results

The experimental results included in the main paper describe a subset of all the considered tasks. In this section, we provide the results of the complete set, along with additional supporting tables and figures.

Performance and fairness violation of Deep Ensemble and individual members. Tab. 3 and Tab. 2 contain the performance and fairness violations of individual ensemble members and the resulting Deep Ensemble, respectively.

The disparate benefits effect for Deep Ensembles. Fig. 8 - 10 depict the change in performance and fairness violations when adding individual ensemble members for all considered tasks.

Changes in PR, TPR and FPR. Fig. 11 - 13 display the change in PR, TPR and FPR per group when adding individual ensemble members for all considered tasks.

Difference in average predictive diversity. Fig. 14 - 16 depict the differences in average predictive diversity per target and protected group.

Hardt post-processing (PP). Tab. 4 - 18 contain the results of mitigating unfairness by means of PP (Hardt et al., 2016) on all considered tasks. PP was either applied with the threshold set to the average fairness violation of the individual ensemble members on the validation set (val) or to 0.05. Note that for some tasks, the original fairness violation of both the Deep Ensemble and its members was already lower than 0.05, where PP leads to an increase in unfairness up to the desired threshold. Experiments on FairFace and CheXpert use the respective validation sets to learn the group dependent thresholds in PP. For experiments on UTKFace, the FairFace validation set was used to learn the thresholds, as it was designed to emulate a real-world distribution shift scenario. Also for UTKFace, the same conclusions as for the FairFace experiments described in the main paper hold, *i.e.*, while PP is very effective to mitigate unfairness in the Deep Ensembles, the desired fairness violation (0.05) is not reached due to the distribution shift. Note that the balanced accuracy was used as the performance metric for CheXpert, because the metric investigated in the main paper, the AUROC, does not consider selecting a threshold.

Table 2: Performance and fairness violations of Deep Ensembles (10 members). Statistics are obtained from five independent runs.

\mathcal{D}'	Target / Group	Accuracy (\uparrow)	SPD (\downarrow)	EOD (\downarrow)	AOD (\downarrow)
FF	age / gender	0.812 \pm 0.007	0.190 \pm 0.009	0.165 \pm 0.010	0.126 \pm 0.008
FF	age / race	0.812 \pm 0.007	0.112 \pm 0.008	0.063 \pm 0.011	0.075 \pm 0.008
FF	gender / age	0.909 \pm 0.004	0.142 \pm 0.003	0.109 \pm 0.005	0.065 \pm 0.004
FF	gender / race	0.909 \pm 0.004	0.009 \pm 0.003	0.003 \pm 0.004	0.004 \pm 0.003
FF	race / age	0.885 \pm 0.004	0.035 \pm 0.003	0.038 \pm 0.014	0.025 \pm 0.006
FF	race / gender	0.885 \pm 0.004	0.005 \pm 0.004	0.025 \pm 0.010	0.015 \pm 0.005
UTK	age / gender	0.793 \pm 0.005	0.309 \pm 0.009	0.252 \pm 0.009	0.204 \pm 0.008
UTK	age / race	0.793 \pm 0.005	0.214 \pm 0.006	0.188 \pm 0.007	0.106 \pm 0.005
UTK	gender / age	0.923 \pm 0.003	0.180 \pm 0.003	0.083 \pm 0.004	0.054 \pm 0.002
UTK	gender / race	0.923 \pm 0.003	0.002 \pm 0.002	0.023 \pm 0.003	0.029 \pm 0.002
UTK	race / age	0.840 \pm 0.006	0.129 \pm 0.004	0.079 \pm 0.008	0.044 \pm 0.005
UTK	race / gender	0.840 \pm 0.006	0.010 \pm 0.004	0.024 \pm 0.008	0.014 \pm 0.004
\mathcal{D}'	Group	AUROC (\uparrow)	SPD (\downarrow)	EOD (\downarrow)	AOD (\downarrow)
CX	age	0.943 \pm 0.001	0.139 \pm 0.002	0.181 \pm 0.006	0.104 \pm 0.003
CX	gender	0.943 \pm 0.001	0.000 \pm 0.001	0.024 \pm 0.006	0.014 \pm 0.003
CX	race	0.943 \pm 0.001	0.040 \pm 0.001	0.092 \pm 0.005	0.048 \pm 0.002

Table 3: Performance and fairness violations of individual members. Statistics are obtained from five independent runs.

\mathcal{D}'	Target / Group	Accuracy (\uparrow)	SPD (\downarrow)	EOD (\downarrow)	AOD (\downarrow)
FF	age / gender	0.794 \pm 0.001	0.173 \pm 0.001	0.153 \pm 0.002	0.113 \pm 0.001
FF	age / race	0.794 \pm 0.001	0.107 \pm 0.004	0.058 \pm 0.004	0.072 \pm 0.004
FF	gender / age	0.899 \pm 0.001	0.142 \pm 0.001	0.114 \pm 0.001	0.068 \pm 0.001
FF	gender / race	0.899 \pm 0.001	0.010 \pm 0.001	0.003 \pm 0.001	0.006 \pm 0.001
FF	race / age	0.873 \pm 0.000	0.040 \pm 0.001	0.040 \pm 0.005	0.029 \pm 0.002
FF	race / gender	0.873 \pm 0.000	0.004 \pm 0.002	0.019 \pm 0.003	0.013 \pm 0.002
UTK	age / gender	0.782 \pm 0.001	0.296 \pm 0.003	0.240 \pm 0.003	0.195 \pm 0.003
UTK	age / race	0.782 \pm 0.001	0.207 \pm 0.002	0.182 \pm 0.003	0.104 \pm 0.002
UTK	gender / age	0.916 \pm 0.001	0.180 \pm 0.002	0.087 \pm 0.003	0.056 \pm 0.001
UTK	gender / race	0.916 \pm 0.001	0.002 \pm 0.001	0.023 \pm 0.002	0.028 \pm 0.001
UTK	race / age	0.822 \pm 0.002	0.118 \pm 0.001	0.073 \pm 0.002	0.043 \pm 0.001
UTK	race / gender	0.822 \pm 0.002	0.008 \pm 0.001	0.021 \pm 0.002	0.015 \pm 0.001
\mathcal{D}'	Group	AUROC (\uparrow)	SPD (\downarrow)	EOD (\downarrow)	AOD (\downarrow)
CX	age	0.940 \pm 0.000	0.138 \pm 0.001	0.174 \pm 0.003	0.101 \pm 0.001
CX	gender	0.940 \pm 0.000	0.000 \pm 0.001	0.024 \pm 0.003	0.014 \pm 0.001
CX	race	0.940 \pm 0.000	0.041 \pm 0.000	0.091 \pm 0.003	0.049 \pm 0.001

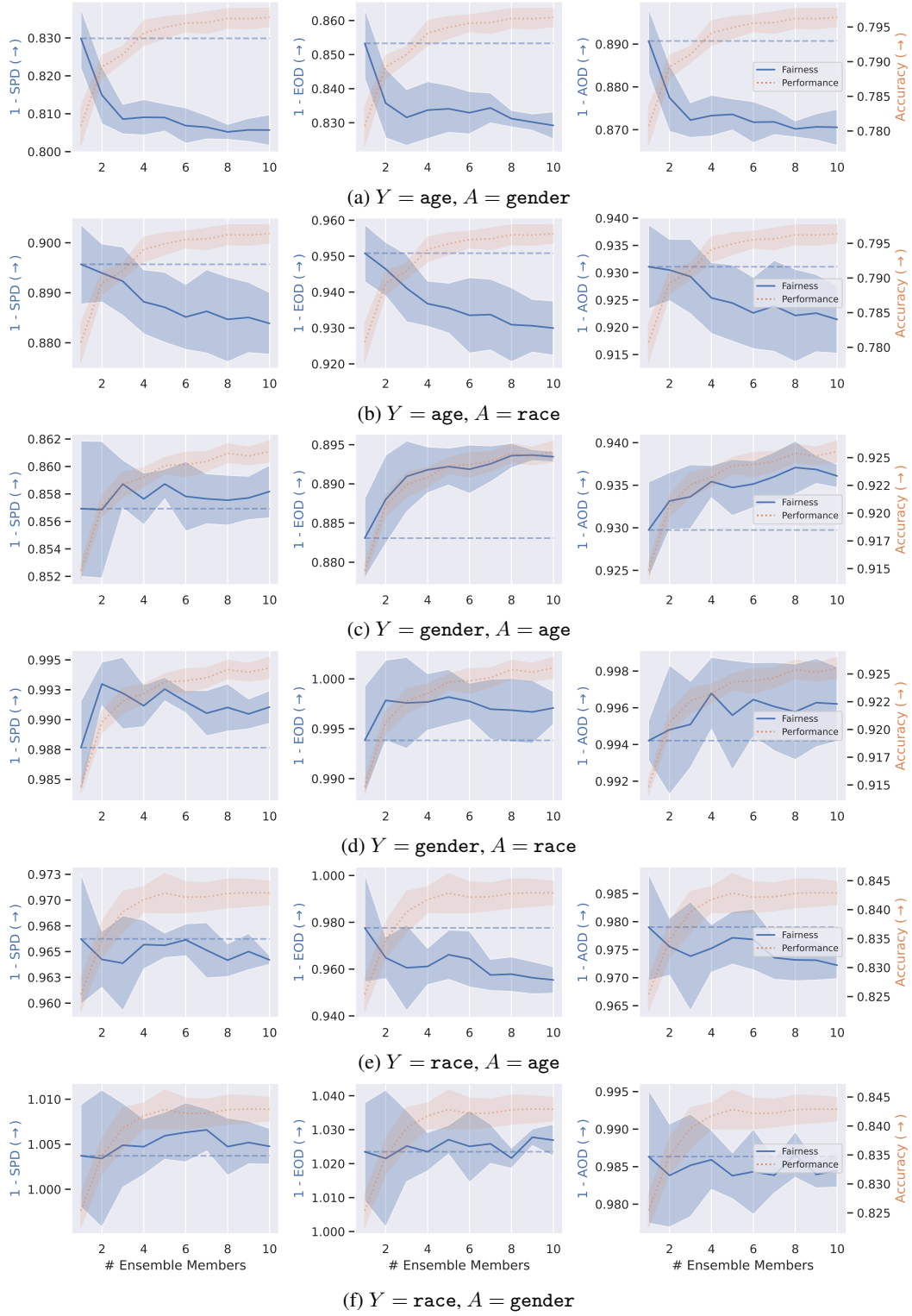


Figure 8: The disparate benefits effect of Deep Ensembles. The **performance** increases, but also the **fairness** changes, often decreasing, when adding more members to the ensemble. Models are trained and evaluated on the FF dataset. Statistics are computed based on five independent runs.

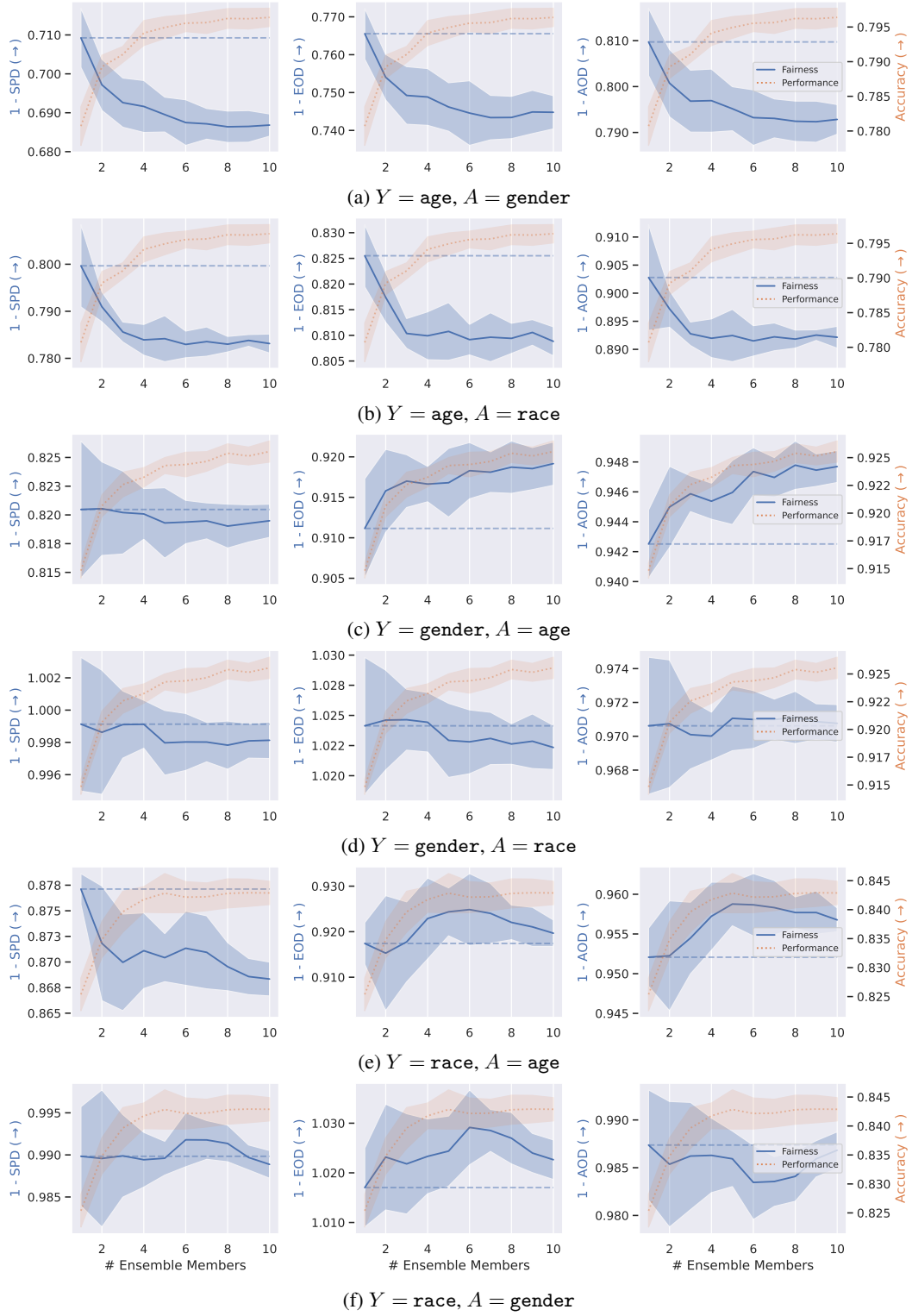


Figure 9: The disparate benefits effect of Deep Ensembles. The performance increases, but also the fairness changes, often decreasing, when adding more members to the ensemble. Models are trained on FF and evaluated on the UTK dataset. Statistics are computed based on five independent runs.

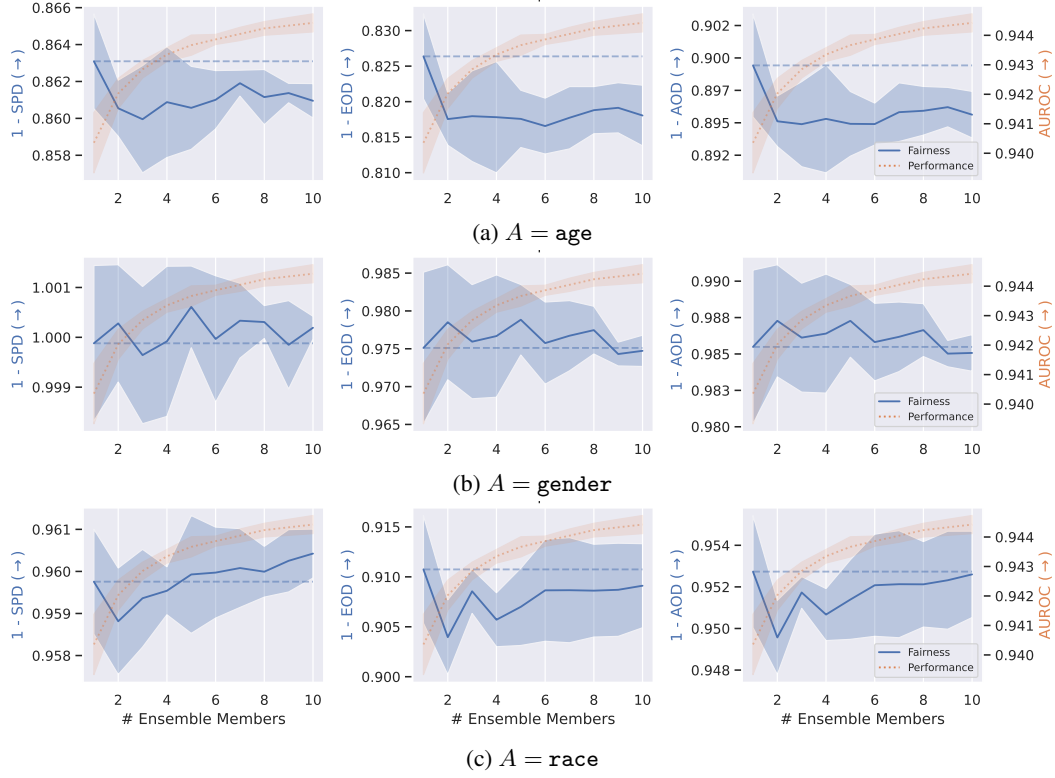


Figure 10: The disparate benefits effect of Deep Ensembles. The **performance** increases, but also the **fairness** changes, often decreasing, when adding more members to the ensemble. Models are trained and evaluated on the CX dataset. Statistics are computed based on five independent runs.

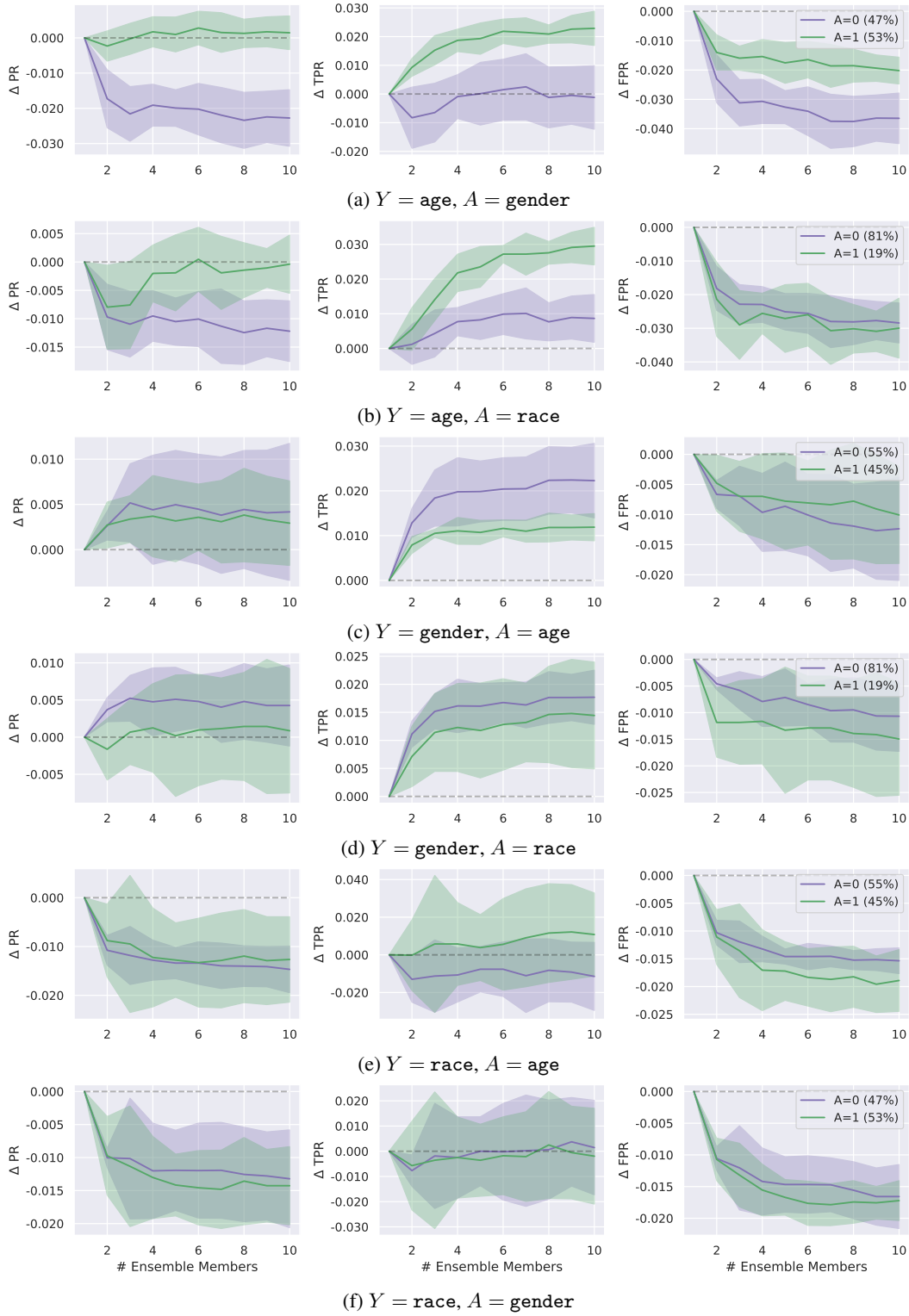


Figure 11: Changes in PR, TPR and FPR on the FF dataset. Statistics are computed based on five independent runs.

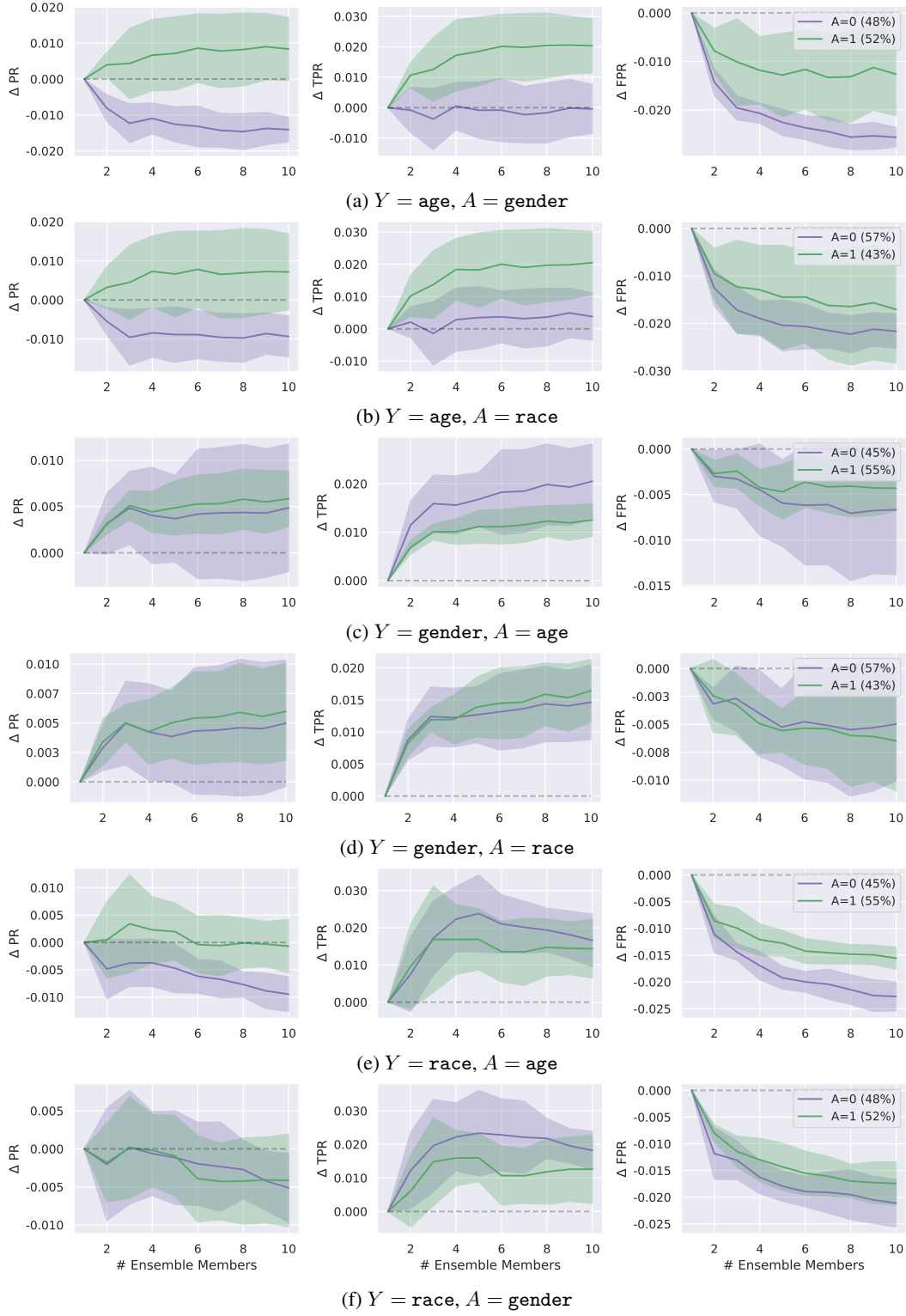


Figure 12: Changes in PR, TPR and FPR on the UTK dataset. Statistics are computed based on five independent runs.

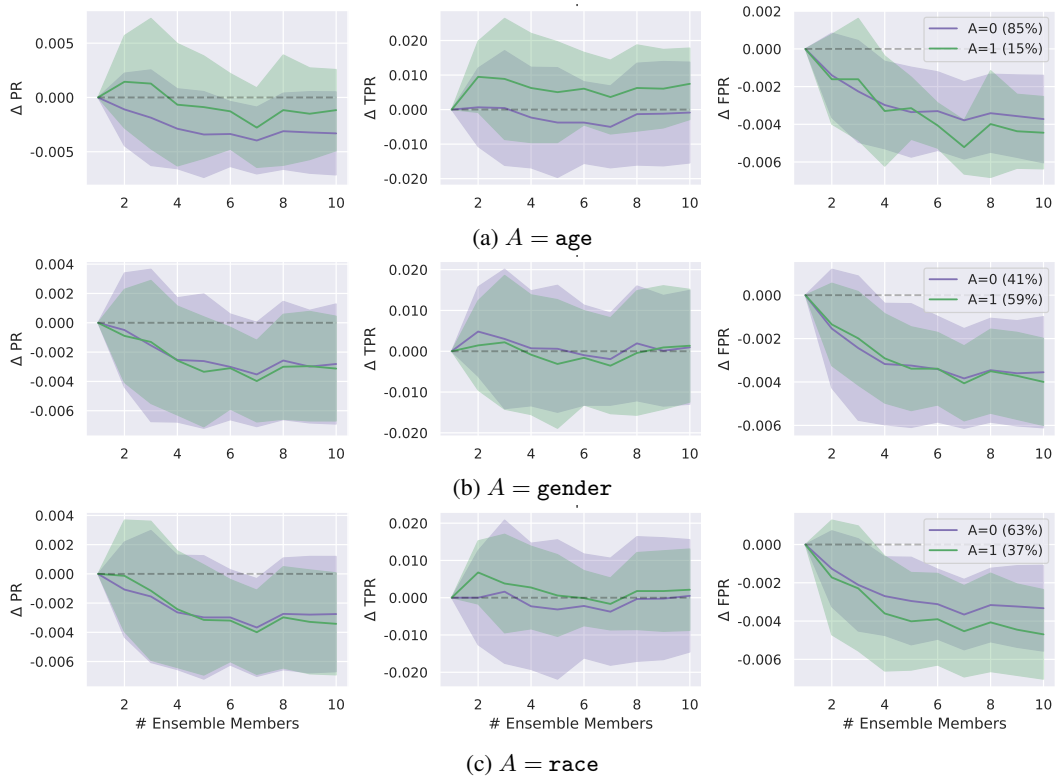


Figure 13: Changes in PR, TPR and FPR on the CX dataset. Statistics are computed based on five independent runs.

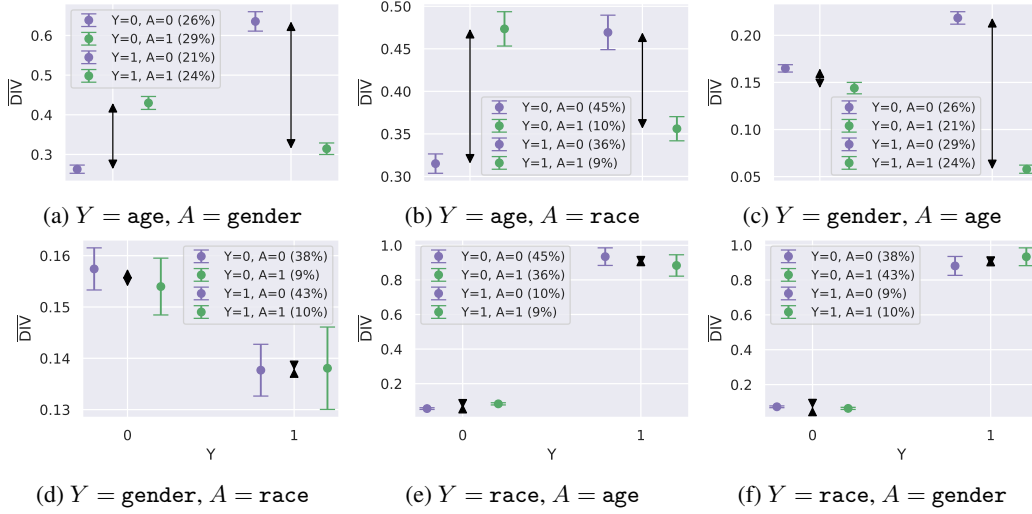


Figure 14: Average predictive diversity \overline{DIV} for each value of the protected attribute A and target variable Y on the FF dataset. Statistics are obtained from five independent runs.

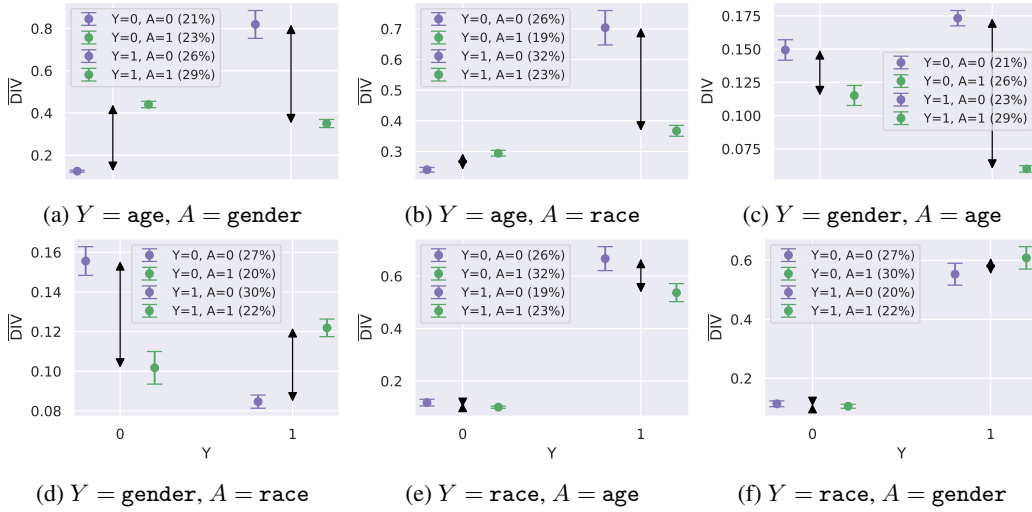


Figure 15: Average predictive diversity \overline{DIV} for each value of the protected attribute A and target variable Y on the UTK dataset. Statistics are obtained from five independent runs.

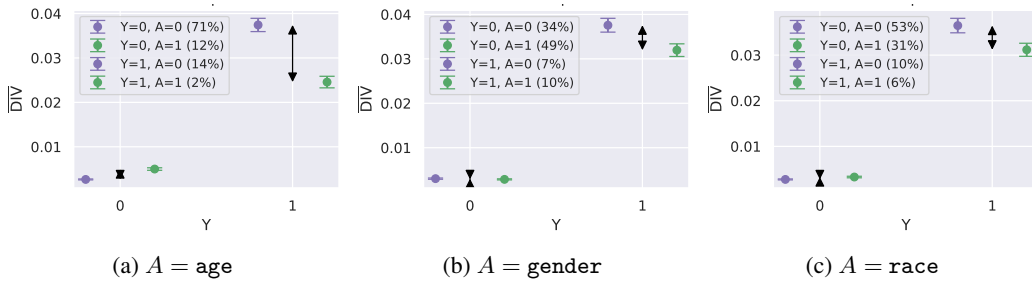


Figure 16: Average predictive diversity \overline{DIV} for each value of the protected attribute A and target variable Y on the CX dataset. Statistics are obtained from five independent runs.

Table 4: PP results (accuracy and fairness violation metrics) on FF. Models are trained on target variable age, evaluated using protected attribute gender. Statistics are obtained from five independent runs, and additionally over all individual ensemble members if applicable.

Before PP	Acc (\uparrow)	SPD (\downarrow)	Acc (\uparrow)	EOD (\downarrow)	Acc (\uparrow)	AOD (\downarrow)
Members	0.794 \pm .003	0.173 \pm .007	0.794 \pm .003	0.153 \pm .012	0.794 \pm .003	0.113 \pm .008
Deep Ensemble	0.816 \pm .002	0.194 \pm .004	0.816 \pm .002	0.171 \pm .004	0.816 \pm .002	0.129 \pm .004
After PP	PP-SPD (\downarrow)		PP-EOD (\downarrow)		PP-AOD (\downarrow)	
Deep Ens. (val)	0.818 \pm .001	0.176 \pm .011	0.818 \pm .001	0.157 \pm .014	0.818 \pm .001	0.114 \pm .012
Deep Ens. (0.05)	0.818 \pm .001	0.057 \pm .003	0.815 \pm .002	0.067 \pm .006	0.816 \pm .002	0.062 \pm .002
Members (0.05)	0.789 \pm .005	0.056 \pm .024	0.792 \pm .005	0.055 \pm .021	0.793 \pm .005	0.054 \pm .015

Table 5: PP results results (accuracy and fairness violation metrics) on FF. Models are trained on target variable age, evaluated using protected attribute race. Statistics are obtained from five independent runs, and additionally over all individual ensemble members if applicable.

Before PP	Acc (\uparrow)	SPD (\downarrow)	Acc (\uparrow)	EOD (\downarrow)	Acc (\uparrow)	AOD (\downarrow)
Members	0.794 \pm .003	0.107 \pm .007	0.794 \pm .003	0.058 \pm .011	0.794 \pm .003	0.072 \pm .007
Deep Ensemble	0.816 \pm .001	0.116 \pm .006	0.816 \pm .001	0.070 \pm .008	0.816 \pm .001	0.079 \pm .006
After PP	PP-SPD (\downarrow)		PP-EOD (\downarrow)		PP-AOD (\downarrow)	
Deep Ens. (val)	0.818 \pm .001	0.070 \pm .011	0.818 \pm .001	0.041 \pm .006	0.818 \pm .001	0.032 \pm .012
Deep Ens. (0.05)	0.818 \pm .001	0.063 \pm .007	0.818 \pm .001	0.033 \pm .013	0.818 \pm .001	0.032 \pm .011
Members (0.05)	0.795 \pm .004	0.061 \pm .015	0.795 \pm .004	0.049 \pm .028	0.795 \pm .004	0.054 \pm .018

Table 6: PP results (accuracy and fairness violation metrics) on FF. Models are trained on target variable gender, evaluated using protected attribute age. Statistics are obtained from five independent runs, and additionally over all individual ensemble members if applicable.

Before PP	Acc (\uparrow)	SPD (\downarrow)	Acc (\uparrow)	EOD (\downarrow)	Acc (\uparrow)	AOD (\downarrow)
Members	0.899 \pm .003	0.142 \pm .005	0.899 \pm .003	0.114 \pm .007	0.899 \pm .003	0.068 \pm .005
Deep Ensemble	0.913 \pm .001	0.142 \pm .002	0.913 \pm .001	0.107 \pm .001	0.913 \pm .001	0.064 \pm .001
After PP	PP-SPD (\downarrow)		PP-EOD (\downarrow)		PP-AOD (\downarrow)	
Deep Ens. (val)	0.913 \pm .001	0.116 \pm .015	0.913 \pm .001	0.084 \pm .015	0.913 \pm .001	0.067 \pm .001
Deep Ens. (0.05)	0.911 \pm .001	0.055 \pm .003	0.913 \pm .001	0.054 \pm .003	0.913 \pm .001	0.067 \pm .001
Members (0.05)	0.894 \pm .004	0.048 \pm .016	0.897 \pm .004	0.048 \pm .013	0.898 \pm .003	0.072 \pm .005

Table 7: PP results (accuracy and fairness violation metrics) on FF. Models are trained on target variable gender, evaluated using protected attribute race. Statistics are obtained from five independent runs, and additionally over all individual ensemble members if applicable.

Before PP	Acc (\uparrow)	SPD (\downarrow)	Acc (\uparrow)	EOD (\downarrow)	Acc (\uparrow)	AOD (\downarrow)
Members	0.899 \pm .003	0.010 \pm .004	0.899 \pm .003	0.003 \pm .005	0.899 \pm .003	0.006 \pm .003
Deep Ensemble	0.913 \pm .001	0.009 \pm .001	0.913 \pm .001	0.003 \pm .002	0.913 \pm .001	0.004 \pm .002
After PP	PP-SPD (\downarrow)		PP-EOD (\downarrow)		PP-AOD (\downarrow)	
Deep Ens. (val)	0.912 \pm .001	0.037 \pm .005	0.912 \pm .001	0.004 \pm .007	0.912 \pm .001	0.007 \pm .001
Deep Ens. (0.05)	0.912 \pm .001	0.009 \pm .002	0.912 \pm .001	0.024 \pm .007	0.912 \pm .001	0.032 \pm .008
Members (0.05)	0.898 \pm .003	0.002 \pm .013	0.898 \pm .003	0.007 \pm .019	0.898 \pm .003	0.017 \pm .012

Table 8: PP results (accuracy and fairness violation metrics) on FF. Models are trained on target variable race, evaluated using protected attribute age. Statistics are obtained from five independent runs, and additionally over all individual ensemble members if applicable.

Before PP	Acc (\uparrow)	SPD (\downarrow)	Acc (\uparrow)	EOD (\downarrow)	Acc (\uparrow)	AOD (\downarrow)
Members	0.873 \pm .002	0.040 \pm .006	0.873 \pm .002	0.040 \pm .017	0.873 \pm .002	0.029 \pm .009
Ensemble	0.888 \pm .001	0.036 \pm .000	0.888 \pm .001	0.045 \pm .006	0.888 \pm .001	0.028 \pm .002
After PP	PP-SPD (\downarrow)		PP-EOD (\downarrow)		PP-AOD (\downarrow)	
Deep Ens. (val)	0.887 \pm .001	0.040 \pm .003	0.888 \pm .001	0.030 \pm .011	0.887 \pm .001	0.025 \pm .006
Deep Ens. (0.05)	0.888 \pm .001	0.052 \pm .004	0.888 \pm .001	0.054 \pm .006	0.887 \pm .001	0.052 \pm .011
Members (0.05)	0.873 \pm .004	0.030 \pm .024	0.873 \pm .004	0.018 \pm .050	0.874 \pm .004	0.038 \pm .030

Table 9: PP results (accuracy and fairness violation metrics) on FF. Models are trained on target variable race, evaluated using protected attribute gender. Statistics are obtained from five independent runs, and additionally over all individual ensemble members if applicable.

Before PP	Acc (\uparrow)	SPD (\downarrow)	Acc (\uparrow)	EOD (\downarrow)	Acc (\uparrow)	AOD (\downarrow)
Members	0.873 \pm .002	0.004 \pm .005	0.873 \pm .002	0.019 \pm .016	0.873 \pm .002	0.013 \pm .006
Ensemble	0.888 \pm .001	0.005 \pm .002	0.888 \pm .001	0.027 \pm .005	0.888 \pm .001	0.016 \pm .002
After PP	PP-SPD (\downarrow)		PP-EOD (\downarrow)		PP-AOD (\downarrow)	
Deep Ens. (val)	0.888 \pm .001	0.012 \pm .003	0.888 \pm .001	0.005 \pm .007	0.888 \pm .001	0.016 \pm .005
Deep Ens. (0.05)	0.888 \pm .002	0.013 \pm .010	0.888 \pm .002	0.017 \pm .022	0.888 \pm .002	0.019 \pm .004
Members (0.05)	0.873 \pm .004	0.004 \pm .025	0.873 \pm .004	0.003 \pm .044	0.873 \pm .004	0.029 \pm .027

Table 10: PP results (accuracy and fairness violation metrics) on UTK. Models are trained on target variable age, evaluated using protected attribute gender. Statistics are obtained from five independent runs, and additionally over all individual ensemble members if applicable.

Before PP	Acc (\uparrow)	SPD (\downarrow)	Acc (\uparrow)	EOD (\downarrow)	Acc (\uparrow)	AOD (\downarrow)
Members	0.782 \pm .004	0.296 \pm .008	0.782 \pm .004	0.240 \pm .012	0.782 \pm .004	0.195 \pm .008
Ensemble	0.796 \pm .001	0.313 \pm .003	0.796 \pm .001	0.255 \pm .004	0.796 \pm .001	0.207 \pm .003
After PP	PP-SPD (\downarrow)		PP-EOD (\downarrow)		PP-AOD (\downarrow)	
Deep Ens. (val)	0.796 \pm .002	0.299 \pm .008	0.796 \pm .002	0.245 \pm .011	0.795 \pm .002	0.194 \pm .010
Deep Ens. (0.05)	0.795 \pm .004	0.211 \pm .005	0.796 \pm .003	0.175 \pm .007	0.797 \pm .004	0.155 \pm .006
Members (0.05)	0.777 \pm .004	0.202 \pm .021	0.778 \pm .004	0.163 \pm .018	0.778 \pm .004	0.145 \pm .013

Table 11: PP results (accuracy and fairness violation metrics) on UTK. Models are trained on target variable age, evaluated using protected attribute race. Statistics are obtained from five independent runs, and additionally over all individual ensemble members if applicable.

Before PP	Acc (\uparrow)	SPD (\downarrow)	Acc (\uparrow)	EOD (\downarrow)	Acc (\uparrow)	AOD (\downarrow)
Members	0.782 \pm .004	0.207 \pm .007	0.782 \pm .004	0.182 \pm .009	0.782 \pm .004	0.104 \pm .007
Deep Ensemble	0.796 \pm .001	0.217 \pm .002	0.796 \pm .001	0.191 \pm .003	0.796 \pm .001	0.108 \pm .002
After PP	PP-SPD (\downarrow)		PP-EOD (\downarrow)		PP-AOD (\downarrow)	
Deep Ens. (val)	0.791 \pm .001	0.188 \pm .008	0.792 \pm .001	0.168 \pm .006	0.791 \pm .001	0.085 \pm .004
Deep Ens. (0.05)	0.791 \pm .001	0.183 \pm .005	0.791 \pm .001	0.163 \pm .010	0.791 \pm .001	0.085 \pm .004
Members (0.05)	0.774 \pm .005	0.173 \pm .011	0.777 \pm .005	0.176 \pm .021	0.777 \pm .005	0.092 \pm .011

Table 12: PP results (accuracy and fairness violation metrics) on UTK. Models are trained on target variable **gender**, evaluated using protected attribute **age**. Statistics are obtained from five independent runs, and additionally over all individual ensemble members if applicable.

Before PP	Acc (\uparrow)	SPD (\downarrow)	Acc (\uparrow)	EOD (\downarrow)	Acc (\uparrow)	AOD (\downarrow)
Members	0.916 \pm .002	0.180 \pm .005	0.916 \pm .002	0.087 \pm .007	0.916 \pm .002	0.056 \pm .003
Deep Ensemble	0.926 \pm .001	0.181 \pm .001	0.926 \pm .001	0.081 \pm .003	0.926 \pm .001	0.052 \pm .001
After PP	PP-SPD (\downarrow)		PP-EOD (\downarrow)		PP-AOD (\downarrow)	
Deep Ens. (val)	0.925 \pm .001	0.161 \pm .011	0.925 \pm .001	0.060 \pm .013	0.925 \pm .001	0.051 \pm .002
Deep Ens. (0.05)	0.920 \pm .001	0.117 \pm .001	0.923 \pm .001	0.037 \pm .002	0.925 \pm .001	0.051 \pm .002
Members (0.05)	0.910 \pm .001	0.111 \pm .011	0.911 \pm .001	0.034 \pm .011	0.914 \pm .001	0.057 \pm .003

Table 13: PP results (accuracy and fairness violation metrics) on UTK. Models are trained on target variable **gender**, evaluated using protected attribute **race**. Statistics are obtained from five independent runs, and additionally over all individual ensemble members if applicable.

Before PP	Acc (\uparrow)	SPD (\downarrow)	Acc (\uparrow)	EOD (\downarrow)	Acc (\uparrow)	AOD (\downarrow)
Members	0.916 \pm .002	0.002 \pm .003	0.916 \pm .002	0.023 \pm .004	0.916 \pm .002	0.028 \pm .003
Deep Ensemble	0.926 \pm .001	0.002 \pm .001	0.926 \pm .001	0.022 \pm .002	0.926 \pm .001	0.029 \pm .001
After PP	PP-SPD (\downarrow)		PP-EOD (\downarrow)		PP-AOD (\downarrow)	
Deep Ens. (val)	0.926 \pm .001	0.021 \pm .003	0.924 \pm .001	0.029 \pm .006	0.925 \pm .001	0.034 \pm .003
Deep Ens. (0.05)	0.924 \pm .001	0.012 \pm .001	0.923 \pm .002	0.049 \pm .007	0.922 \pm .002	0.053 \pm .005
Members (0.05)	0.914 \pm .002	0.006 \pm .010	0.914 \pm .002	0.035 \pm .015	0.914 \pm .002	0.039 \pm .013

Table 14: PP results (accuracy and fairness violation metrics) on UTK. Models are trained on target variable **race**, evaluated using protected attribute **age**. Statistics are obtained from five independent runs, and additionally over all individual ensemble members if applicable.

Before PP	Acc (\uparrow)	SPD (\downarrow)	Acc (\uparrow)	EOD (\downarrow)	Acc (\uparrow)	AOD (\downarrow)
Members	0.822 \pm .006	0.118 \pm .009	0.822 \pm .006	0.073 \pm .016	0.822 \pm .006	0.043 \pm .007
Deep Ensemble	0.843 \pm .002	0.132 \pm .002	0.843 \pm .002	0.080 \pm .003	0.843 \pm .002	0.043 \pm .002
After PP	PP-SPD (\downarrow)		PP-EOD (\downarrow)		PP-AOD (\downarrow)	
Deep Ens. (val)	0.857 \pm .001	0.131 \pm .006	0.858 \pm .002	0.066 \pm .008	0.858 \pm .002	0.042 \pm .003
Deep Ens. (0.05)	0.856 \pm .002	0.149 \pm .007	0.858 \pm .002	0.086 \pm .005	0.857 \pm .003	0.057 \pm .006
Members (0.05)	0.816 \pm .014	0.118 \pm .038	0.816 \pm .015	0.078 \pm .047	0.817 \pm .014	0.055 \pm .029

Table 15: PP results (accuracy and fairness violation metrics) on UTK. Models are trained on target variable **race**, evaluated using protected attribute **gender**. Statistics are obtained from five independent runs, and additionally over all individual ensemble members if applicable.

Before PP	Acc (\uparrow)	SPD (\downarrow)	Acc (\uparrow)	EOD (\downarrow)	Acc (\uparrow)	AOD (\downarrow)
Members	0.822 \pm .006	0.008 \pm .010	0.822 \pm .006	0.021 \pm .019	0.822 \pm .006	0.015 \pm .010
Ensemble	0.843 \pm .002	0.011 \pm .002	0.843 \pm .002	0.023 \pm .004	0.843 \pm .002	0.013 \pm .002
After PP	PP-SPD (\downarrow)		PP-EOD (\downarrow)		PP-AOD (\downarrow)	
Deep Ens. (val)	0.858 \pm .003	0.039 \pm .002	0.858 \pm .001	0.000 \pm .006	0.859 \pm .003	0.016 \pm .008
Deep Ens. (0.05)	0.859 \pm .002	0.038 \pm .013	0.859 \pm .002	0.019 \pm .019	0.859 \pm .002	0.019 \pm .006
Members (0.05)	0.816 \pm .014	0.009 \pm .044	0.816 \pm .015	0.002 \pm .049	0.816 \pm .014	0.030 \pm .032

Table 16: PP results (balanced accuracy and fairness violation metrics) on CX. Models are evaluated using protected attribute age. Statistics are obtained from five independent runs, and additionally over all individual ensemble members if applicable.

Before PP	BAcc (\uparrow)	SPD (\downarrow)	BAcc (\uparrow)	EOD (\downarrow)	BAcc (\uparrow)	AOD (\downarrow)
Members	0.783 \pm .008	0.138 \pm .004	0.783 \pm .008	0.174 \pm .010	0.783 \pm .008	0.101 \pm .006
Deep Ensemble	0.786 \pm .004	0.139 \pm .001	0.786 \pm .004	0.182 \pm .004	0.786 \pm .004	0.104 \pm .002
After PP	PP-SPD (\downarrow)		PP-EOD (\downarrow)		PP-AOD (\downarrow)	
Deep Ens. (val)	0.801 \pm .004	0.122 \pm .019	0.800 \pm .004	0.125 \pm .048	0.800 \pm .005	0.073 \pm .030
Deep Ens. (0.05)	0.788 \pm .004	0.057 \pm .002	0.798 \pm .005	0.052 \pm .007	0.800 \pm .005	0.038 \pm .010
Members (0.05)	0.782 \pm .010	0.060 \pm .005	0.789 \pm .010	0.063 \pm .015	0.790 \pm .011	0.049 \pm .009

Table 17: PP results (balanced accuracy and fairness violation metrics) on CX. Models are evaluated using protected attribute gender. Statistics are obtained from five independent runs, and additionally over all individual ensemble members if applicable.

Before PP	BAcc (\uparrow)	SPD (\downarrow)	BAcc (\uparrow)	EOD (\downarrow)	BAcc (\uparrow)	AOD (\downarrow)
Members	0.783 \pm .008	0.000 \pm .002	0.783 \pm .008	0.024 \pm .010	0.783 \pm .008	0.014 \pm .005
Deep Ensemble	0.786 \pm .004	0.000 \pm .000	0.786 \pm .004	0.025 \pm .002	0.786 \pm .004	0.015 \pm .001
After PP	PP-SPD (\downarrow)		PP-EOD (\downarrow)		PP-AOD (\downarrow)	
Deep Ens. (val)	0.801 \pm .006	0.002 \pm .001	0.798 \pm .007	0.005 \pm .020	0.798 \pm .007	0.014 \pm .005
Deep Ens. (0.05)	0.796 \pm .005	0.001 \pm .014	0.798 \pm .006	0.009 \pm .024	0.796 \pm .005	0.020 \pm .013
Members (0.05)	0.792 \pm .012	0.001 \pm .013	0.792 \pm .012	0.018 \pm .027	0.792 \pm .012	0.022 \pm .013

Table 18: PP results (balanced accuracy and fairness violation metrics) on CX. Models are evaluated using protected attribute race. Statistics are obtained from five independent runs, and additionally over all individual ensemble members if applicable.

Before PP	BAcc (\uparrow)	SPD (\downarrow)	BAcc (\uparrow)	EOD (\downarrow)	BAcc (\uparrow)	AOD (\downarrow)
Members	0.783 \pm .008	0.041 \pm .002	0.783 \pm .008	0.091 \pm .008	0.783 \pm .008	0.049 \pm .004
Deep Ensemble	0.786 \pm .004	0.040 \pm .001	0.786 \pm .004	0.091 \pm .004	0.786 \pm .004	0.047 \pm .002
After PP	PP-SPD (\downarrow)		PP-EOD (\downarrow)		PP-AOD (\downarrow)	
Deep Ens. (val)	0.801 \pm .007	0.037 \pm .002	0.802 \pm .007	0.083 \pm .010	0.802 \pm .007	0.044 \pm .006
Deep Ens. (0.05)	0.802 \pm .007	0.039 \pm .004	0.802 \pm .008	0.078 \pm .008	0.799 \pm .004	0.053 \pm .013
Members (0.05)	0.793 \pm .011	0.038 \pm .006	0.793 \pm .011	0.073 \pm .019	0.793 \pm .011	0.047 \pm .016

F Additional Investigations

This section presents additional investigations that are complementary to those presented in the main section of the manuscript. First, we investigate how the disparate benefits effect behaves for different model sizes of the individual ensemble members. Second, we conduct the same investigation on different model architectures. Third, we study whether the disparate benefits effect also occurs for heterogeneous Deep Ensembles composed of members with different model architectures. Fourth, we report an alternative approach to mitigate the negative impact on fairness due to Deep Ensembling by means of weighting individual members differently in the ensemble. Finally, we study the sensitivity of the Deep Ensemble and its individual members to the threshold used to make the prediction.

F.1 Model Size

The experiments in the main paper were conducted using ResNet50 models. In this section we investigate whether the size of the models plays a major role in determining the existence and strength of the disparate benefits effect. The results are shown in Fig. 17 - 19. As seen in the Figures, in the majority of cases the performance gains due to ensembling slightly increase for larger model classes. The fairness violations however increase to a larger degree, see *e.g.* Fig. 17 (a) and (b), Fig. 18 (a), (b) and (c) as well as Fig. 19 (a). Generally, we observe an increase in the magnitude of the change in fairness violations with larger model classes for all tasks that exhibit significant disparate benefits (*c.f.* Tab. 1).

F.2 Model Architecture

In this section we investigate the role of the specific model architecture on the existence and strength of the disparate benefits effect. The results are shown in Fig. 20 - 22. In the majority of cases, disparate benefits occur throughout all considered model architectures. Especially for EfficientNetV2-S we observe significant disparate benefits for some cases where we do not observe them in the main investigation based on ResNet50. For example for UTK, target race, group age under AOD (Fig. 21e) or CX, group race under EOD and AOD. Overall, we do not find a systematic difference of the results for different model architectures.

F.3 Heterogenous Ensembles

The results presented in Fig. 1 in the main paper are obtained from a homogeneous Deep Ensemble composed of ResNet50 models. The results presented in Fig. 23 consider the same target / protected group combinations for the same datasets using a heterogeneous Deep Ensemble of ResNet18/34/50 models. We observe the disparate benefits effect for heterogeneous ensembling to a similar extent than for homogeneous ensembling.

F.4 Deep Ensemble Weighting

In this section, we study whether there exist weightings to combine the individual models in the Deep Ensemble that perform better than a standard uniform averaging as in Eq. (1). The approximation in Eq. (1) thus changes to

$$p_{\lambda}(y \mid \mathbf{x}, \mathcal{D}) \approx \sum_{n=1}^N \lambda_n p(y \mid \mathbf{x}, \mathbf{w}_n). \quad (16)$$

λ satisfies $\sum_{n=1}^N \lambda_n = 1$ and $\lambda_n \geq 0 \forall n$. Note that Eq. (16) results in Eq. (1) if $\lambda_n = 1/N \forall n$. We consider $\lambda \sim \text{Dir}(\alpha_1, \dots, \alpha_N)$ with $\alpha_n = 1 \forall n$. Weightings are thus drawn uniformly at random from a $N - 1$ dimensional probability simplex. In our empirical investigation, we sampled 2,000 weightings λ and evaluated the resulting ensembles on the three tasks. The results are given in Fig. 24, showing individual members and the different resulting ensembles, as well as their convex hull. In the case of the FF and UTK datasets, there appears to be a strong correlation between fairness violations and performance, and the weights hardly provide more Pareto optimal models. However, regarding the CX dataset, we observe that there are many weightings that would yield a more favorable outcome than uniform averaging as generally done by Deep Ensembles. In the following, we outline two methods to choose such a weighting. However, both methods did no lead

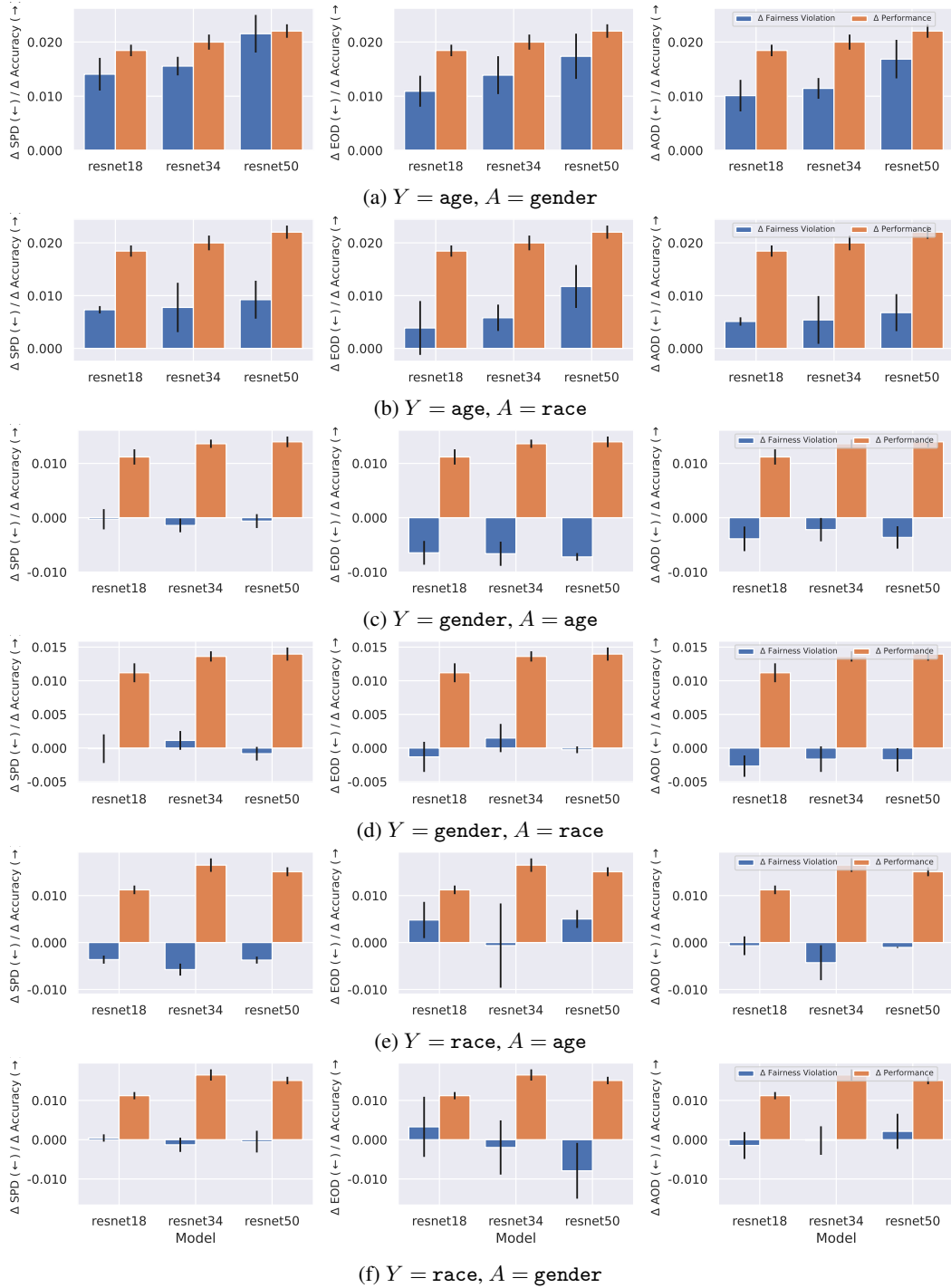


Figure 17: The disparate benefits effect of Deep Ensembles for different model sizes. Models are trained and evaluated on the FF dataset. Statistics are computed based on five independent runs.

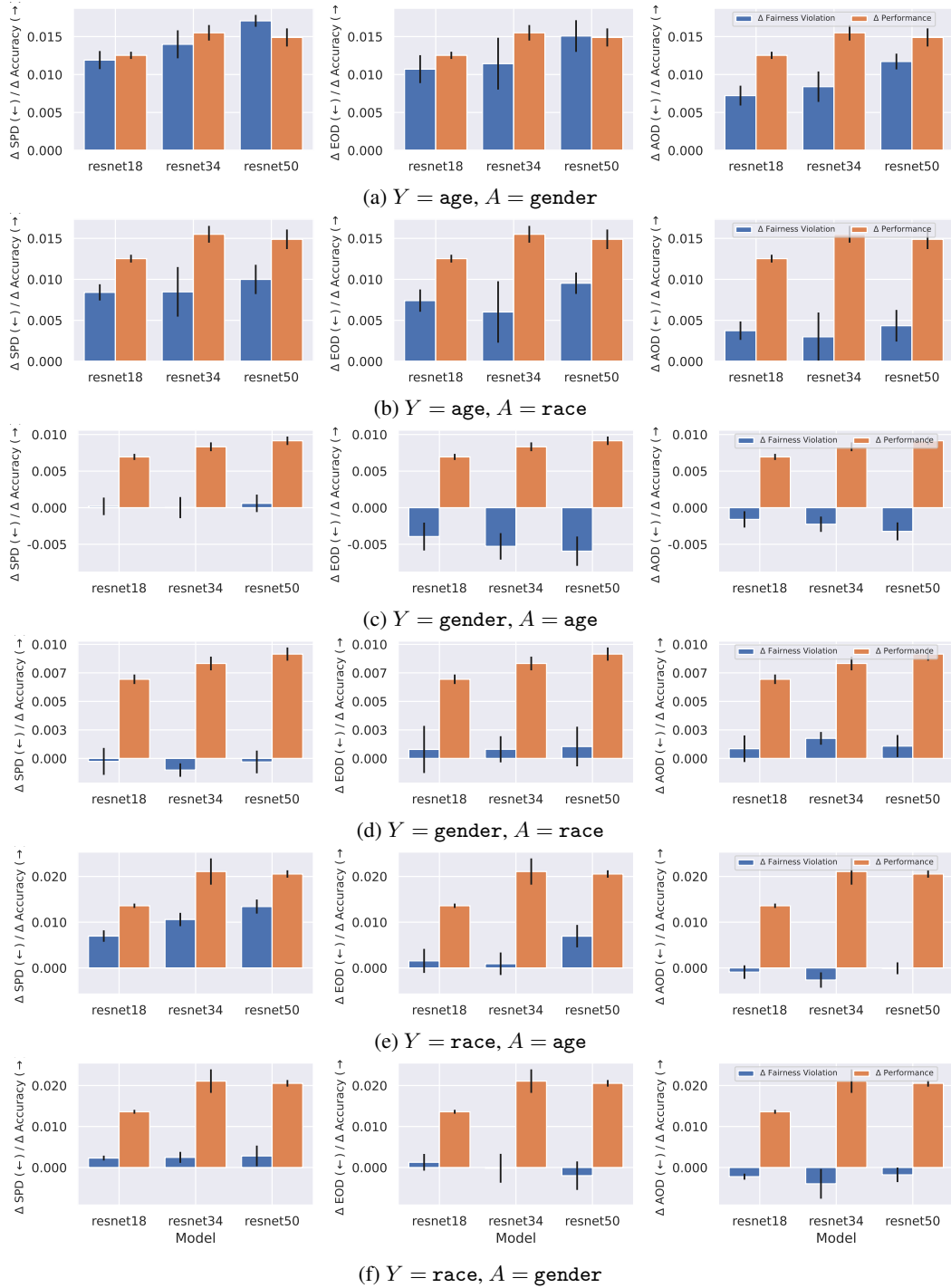


Figure 18: The disparate benefits effect of Deep Ensembles for different model sizes. Models are trained and evaluated on the UTK dataset. Statistics are computed based on five independent runs.

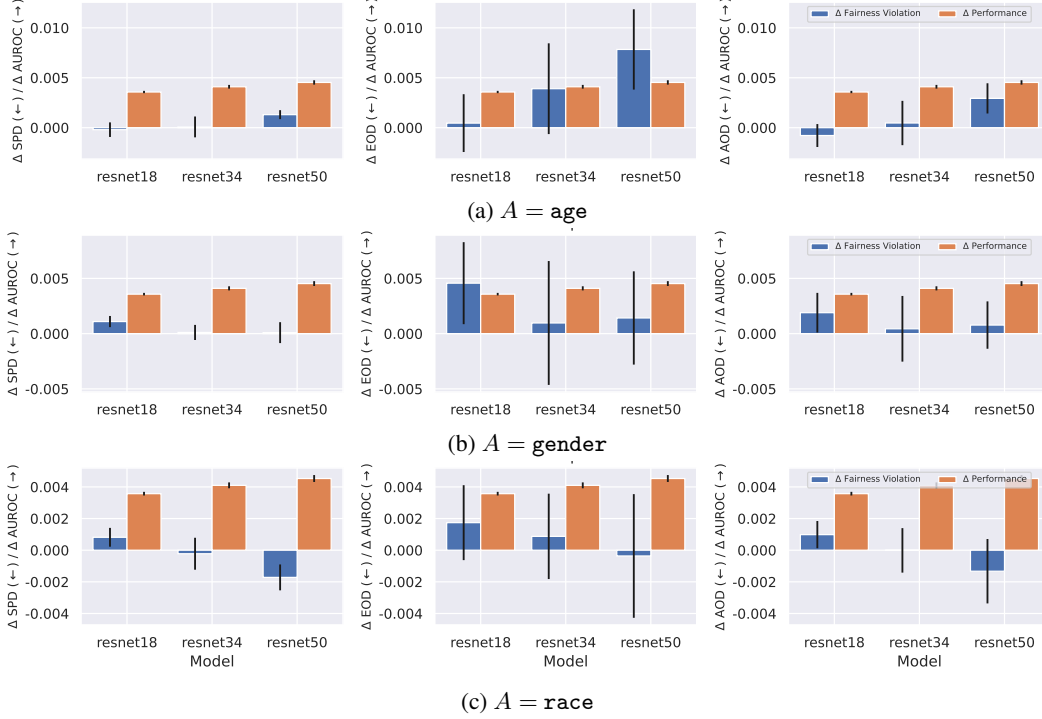


Figure 19: The disparate benefits effect of Deep Ensembles for different model sizes. Models are trained and evaluated on the CX dataset. Statistics are computed based on five independent runs.

to a significantly better outcome than uniform averaging. Nevertheless, we include a qualitative discription of our experiments as guidance for future research.

Weight selection based on the validation set. The simplest approach to identify a more favorable set of weights consists of selecting it as a hyperparameter. In our experiments, we sampled λ uniformly at random as described before and selected the Pareto optimal weighting on the validation set. However, we found that the selected weights did not improve performance on the test dataset, neither for the UTK dataset - where it could expected due to the distribution shift - nor on the FF and CX datasets, where the validation and test datasets are drawn from the same distribution. Notably, the selected solutions were very close to the uniform weighting that is usually used in Deep Ensembles.

Fairness-based weighting. Furthermore, we leveraged the information about the fairness violation of the individual members to define the weights and yield a fairer ensembling. Given a fairness violation measure $F_n \in [0, 1]$ for each ensemble member, we define the weighting factor

$$\lambda_n = \frac{\exp\{-F_n/\tau\}}{\sum_{j=1}^N \exp\{-F_j/\tau\}}, \quad (17)$$

for Eq. (16), where $\tau \in \mathbb{R}_+$ is a temperature hyperparameter. For high values of the temperature parameter $\tau \rightarrow \infty$, Eq. (16) becomes equivalent to Eq. (1). For low values of the temperature parameter $\tau \rightarrow 0$, the fairness-weighted predictive distribution given by Eq. (16) approaches the predictive distribution of the model with lowest fairness violation. We calculated the fairness measure on an additional held out “fairness” dataset. The temperature parameter was selected on the validation dataset. In our experiments, the proposed fairness-weighted Deep Ensemble was not significantly Pareto dominant to the uniform weighting. Notably, the selected solutions were either close to the individual models or to uniform averaging, thus exhibiting extremely high variance. In further analysis, we found that performance and fairness violations are extremely dependent on the selected temperature, both being non-smooth functions of the temperature. On the considered datasets and models, the best temperatures were usually found around $1e-2$.

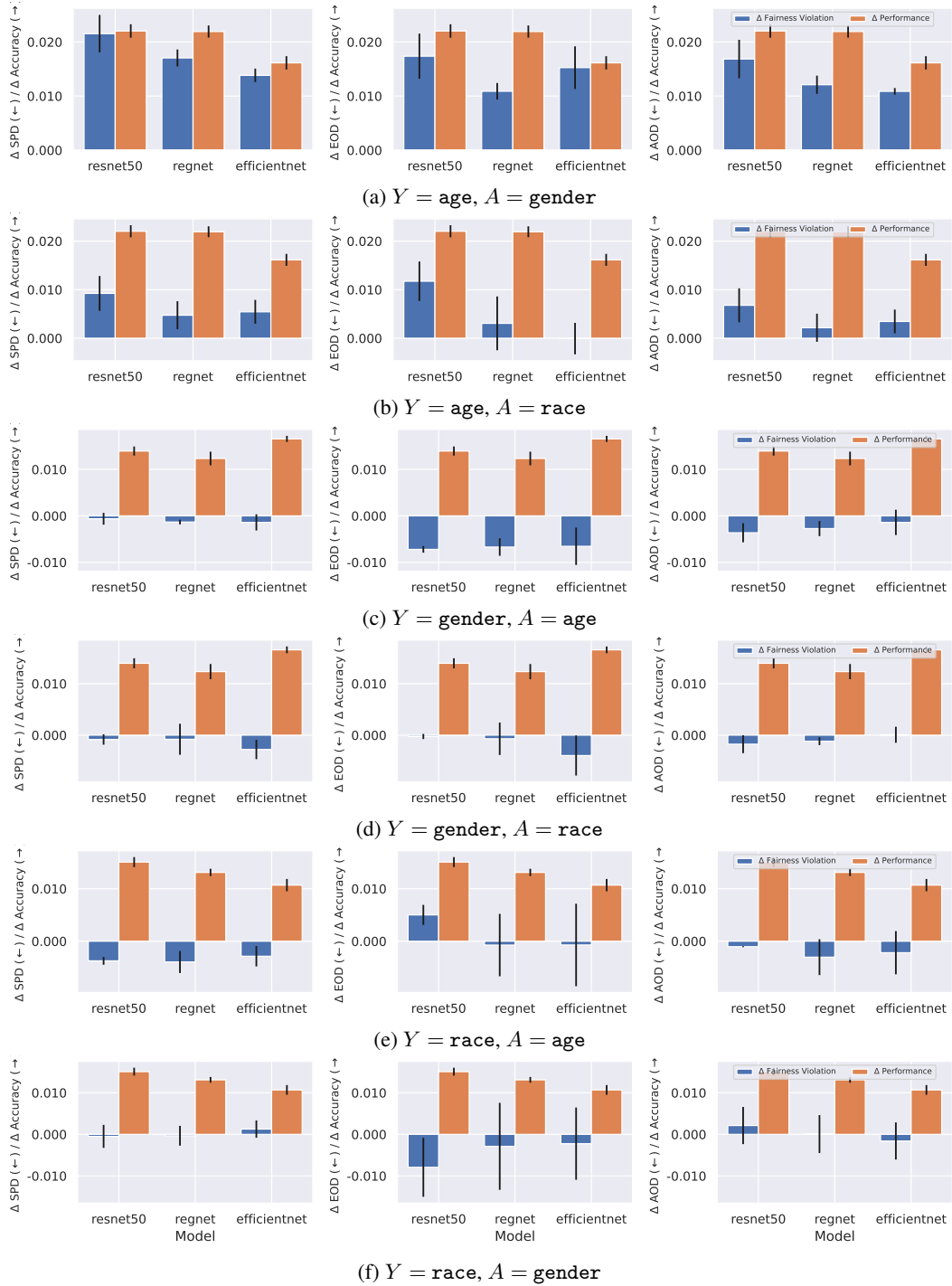


Figure 20: The disparate benefits effect of Deep Ensembles for different model architectures. Models are trained and evaluated on the FF dataset. Statistics are computed based on five independent runs.

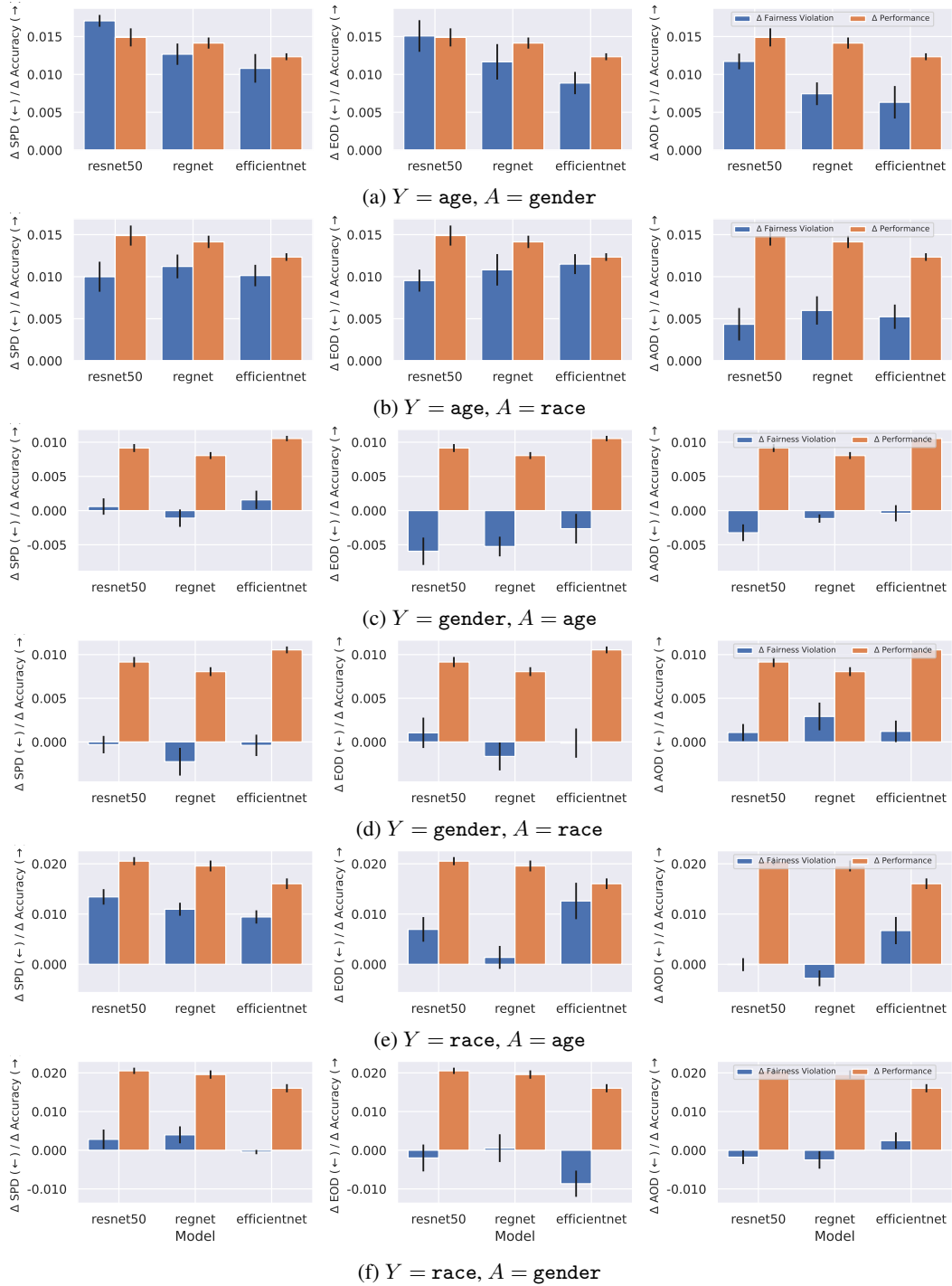


Figure 21: The disparate benefits effect of Deep Ensembles for different model architectures. Models are trained and evaluated on the UTK dataset. Statistics are computed based on five independent runs.

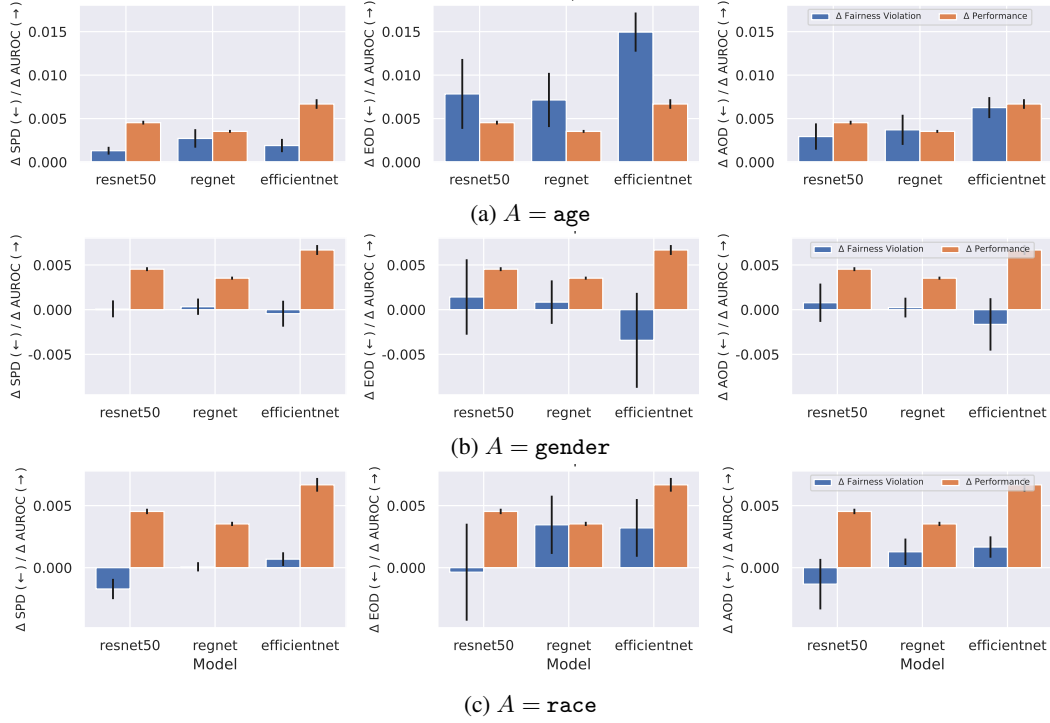


Figure 22: The disparate benefits effect of Deep Ensembles for different model architectures. Models are trained and evaluated on the CX dataset. Statistics are computed based on five independent runs.

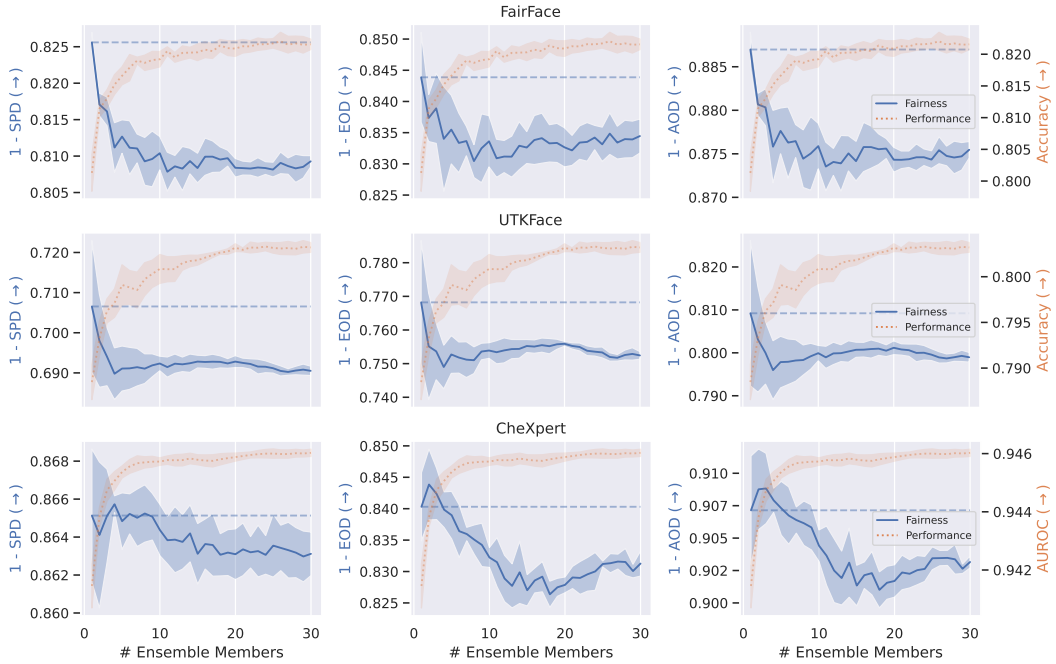


Figure 23: The dangers of the *disparate benefits* effect for heterogeneous (ResNet18/34/50) Deep Ensembles. The **performance** increases, but the **fairness** decreases when adding members to the ensemble. The models evaluated on the FairFace test dataset and UTKFace dataset are trained to predict age as the target variable and are evaluated using gender (male / female) as the protected attribute to define the groups. CheXpert models are trained to predict whether there was a finding regarding a set of medical conditions or not and are evaluated using age (young / old) as the protected attribute to define the groups. Statistics are obtained from five independent runs.

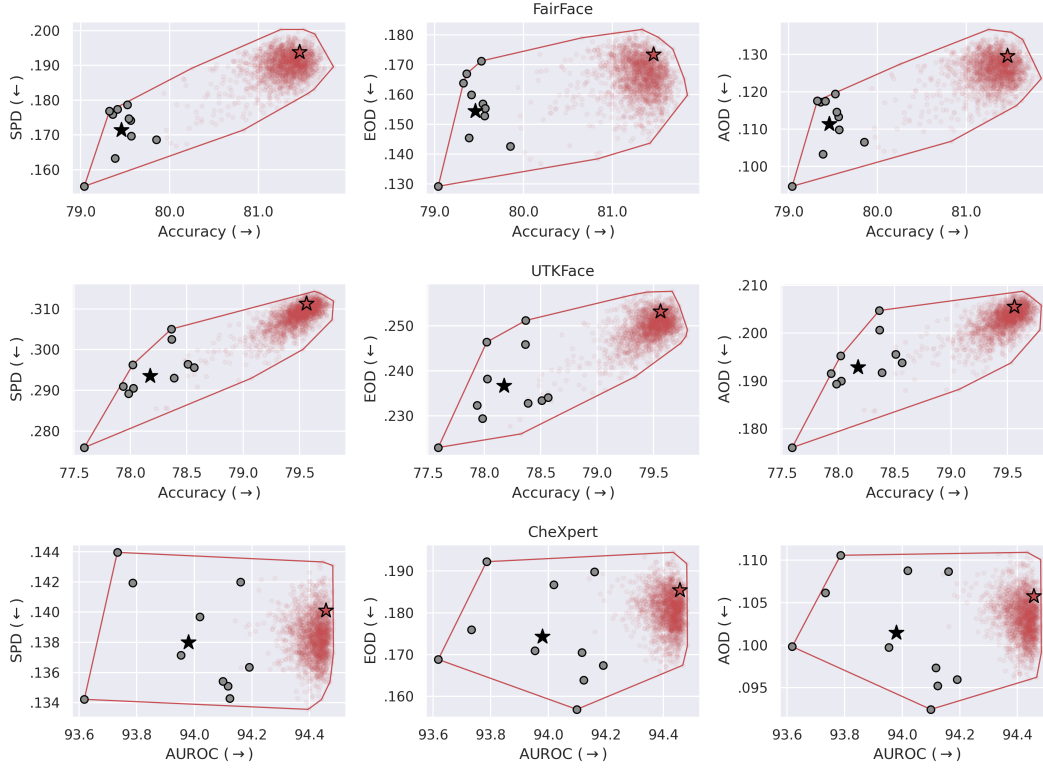


Figure 24: Convex hull of performance and fairness violations for possible weightings to aggregate members of the Deep Ensemble. Ensemble weights are drawn uniformly at random from a $N - 1$ dimensional simplex. Grey points represent individual models, the black star corresponds to their average performance and fairness violation. The red star represents the standard Deep Ensemble with uniform weighting.

F.5 Thresholds Selection

Finally, we report the results of analyzing the dependency of the Deep Ensemble and individual ensemble members on selecting the threshold for prediction. When using the usual `argmax`, implicitly a threshold of 0.5 is used. In the post-processing experiments, we found that applying the method even under an additional fairness constraint can improve the performance. We evaluated all trained models on their respective validation datasets. The results are depicted in Fig. 25. The results show that the Deep Ensemble is more sensitive to the threshold on the FF dataset, especially for target variable age. Regarding the CX dataset, the balanced accuracy exhibits roughly the same behavior under varying thresholds for the Deep Ensemble than for individual members. However, the spread of the optimal threshold is much smaller throughout all experiments.

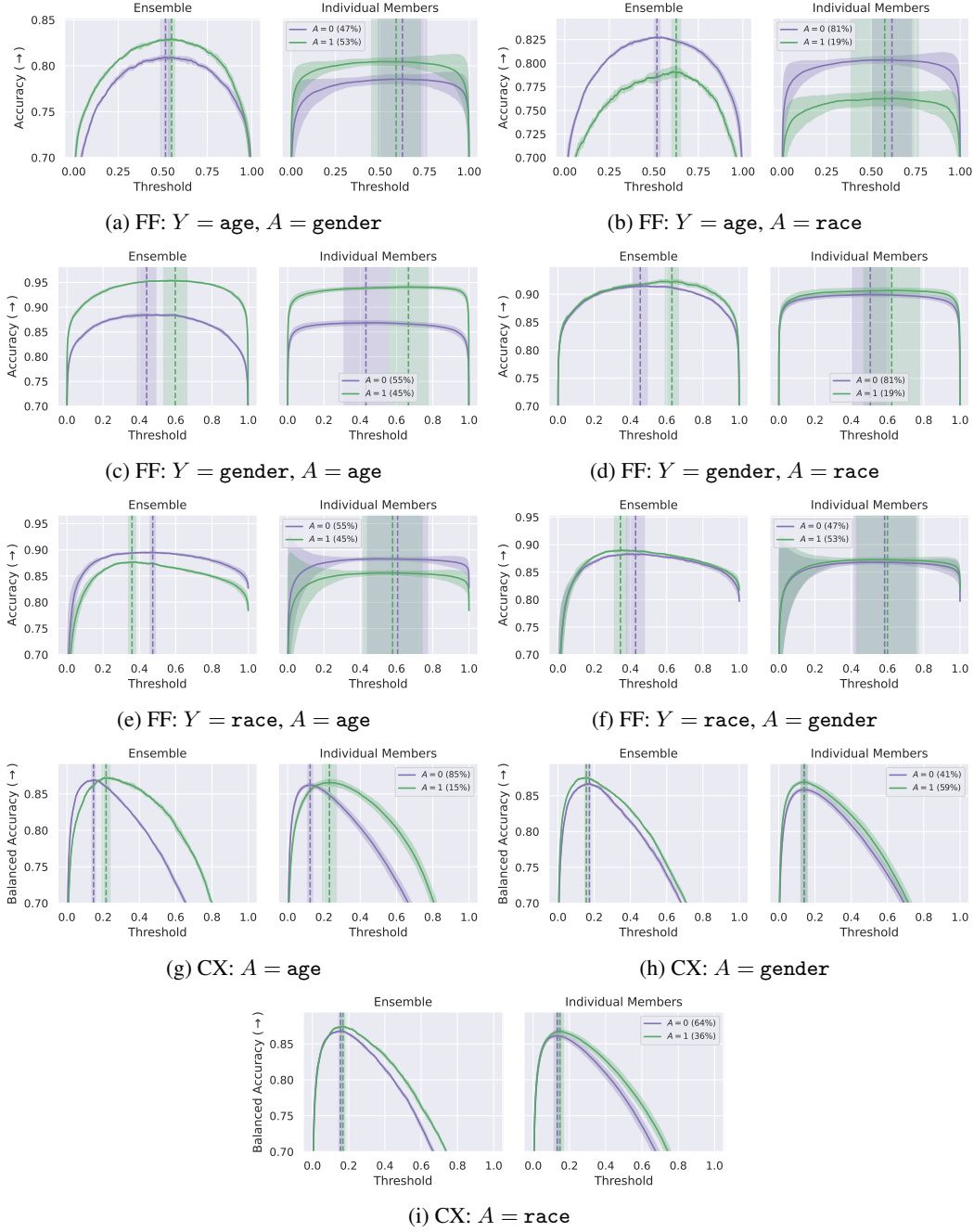


Figure 25: (Balanced) Accuracy depending on the chosen threshold for the FF and CX validation datasets. Vertical lines and shading denote optimal threshold per protected group. Statistics are computed based on five independent runs.